Addis Ababa University

Addis Ababa Institute of Technology (AAiT)

Department of Electrical and Computer Engineering

Speed Control of Vector Controlled PMSM Drive using Fuzzy Logic-PI Controller

A thesis submitted to the School of Graduate Studies in partial fulfilment of the requirement for the degree of Master of Science in Electrical and Computer Engineering

By

Mahlet Legesse Gebresilassie

Advisor:

Professor Wolde-Ghiorgis, Woldemariam

August, 2011

Addis Ababa University

Addis Ababa Institute of Technology (AAiT)

Department of Electrical and Computer Engineering

"Speed Control of Vector Controlled PMSM Drive using Fuzzy Logic- PI Controller"

By

Mahlet Legesse

Electrical and Computer Engineering Department

Approval by Board Examiners

Dr. Getahun Mekuria Chairman, Department Graduate Committee	_____ Signature	_____ Date
Professor Wolde-Ghiorgis, Woldemariam Advisor	_____ Signature	_____ Date
Dr. Mengesha Mamo Internal Examiner	_____ Signature	_____ Date
Prof. Girma Mulissa External Examiner	_____ Signature	_____ Date

Declaration

I, the undersigned declare that this thesis is my original work, and has not been presented for a degree in this or any other university, and all sources of materials used for the thesis have been fully acknowledged.

Mahlet Legesse	_____
Name	Signature
Addis Ababa, Ethiopia	August, 2011
Place	Date of submission

This thesis has been submitted with my approval as a university advisor

Professor. Wolde-ghiorgis Woldemariam	_____
Advisor Name	Signature

ACKNOWLEDGMENTS

I want to start expressing a sincere acknowledgement to my advisor, Professor Wolde-Ghiorgis, Woldemariam for giving me the opportunity to research under his guidance and supervision. I received motivation, comments, encouragement and continuous guidance from him during my graduate studies.

My thanks are extended to my fellow colleagues in Electrical Engineering, especially in the control engineering stream, Solomon W/Tsadik, Zelalem Abay, and Yoseph Tesfaye who built an academic and very friendly study environment that made my study at the university most enjoyable and skilful.

I would like to express my gratitude to my family and particularly to my uncle Eng. Girmay Teklehaimanot for his constant support and my beloved husband, Shambel Aregay, whose love and encouragement have been so strategic in completing this thesis.

I also wish to thank Ato Musse W/Michael and my brother Yeasef Legesse for thier support throughout the thesis. Lastly, a special thanks to W/t Atsede Yaregal for her help during my graduate studies and Meaza Gebrehiwot, and Ato Alemseged who helped me in editing and printing the documentation.

And to the Father Almighty, may you continue to give me strength and vision that I may follow your path…..to eternal salvation.

Mahlet Legesse

TABLE OF CONTENTS

ACKNOWLEDGMENTS ..... **I**
LIST OF FIGURES ..... **V**
LIST OF TABLES ..... **VII**
LIST OF ABBREVIATIONS AND SYMBOLS ..... **VIII**
ABSTRACT ..... **IX**
1. INTRODUCTION **1**
1.1 Background Theory 1
1.2 Motivation 1
1.3 Objective of the Study and Methodology 2
1.3.1 General Objective 2
1.3.2 Specific Objectives 3
1.3.3 Methodology 3
1.4 Literature review 4
1.5 Thesis Organization 6
2. PMSM AND ITS PRINCIPLE OF OPERATION **7**
2.1 Introduction to Synchronous Motor 7
2.2 Permanent Magnet Synchronous Motor 9
2.2.1 Permanent Magnet Materials 10
2.2.2 Classification of Permanent Magnet Motors 10
2.2.2.1 Magnetization of PMs 10
2.2.2.2 Direction of Field Flux 11
2.2.2.3 Flux Density Distribution 11
2.2.2.4 Permanent Magnet Radial Field Motors 12
2.3 Starting Characteristics of PMSM 14
2.4 Why concentrate this study on PMSM? 15
2.5 Applications 16
3. DYNAMIC MODELING OF PMSM DRIVE **17**
3.1 Field Oriented Control (FOC) 17
3.2 Reference frame Transformation (3-Φ to 2-Φ Transformations) 19

3.3 Modeling of PMSM 22
3.3.1 Voltage Equation 22
3.3.2 Equivalent Circuits 23
3.3.3 Power Equivalence 23
3.3.4 Electromagnetic Torque Equation 24
3.3.5 Steady State Torque Characteristics of SPMSM 26
3.3.6 Voltage Decoupling Control 27
4. CONTROL OF PMSM DRIVES 30
4.1 PMSM Drive System 30
4.2 Inverters and Their Control 31
4.2.1 Power Devices 31
4.2.2 DC Input Source 32
4.2.3 Voltage Source Three-Phase Inverter 32
4.3 Position Sensor 35
4.3.1 Optical Encoder 35
4.4 Pulse Width Modulation (PWM) 36
4.4.1 Sinusoidal Pulse width Modulation 36
4.4.2 Space Vector PWM 37
4.5 Controller Design 47
4.5.1 Introduction to Fuzzy-Logic 47
4.5.2 Fuzzy Logic Controller (FLC) 50
4.5.3 PI Controller 55
4.5.4 Fuzzy Logic based self tuning PI Controller 56
4.5.5 Design of Current Controller 61
4.5.5.1 Introduction 61
4.5.5.2 i_q's PI controller design 61
4.5.5.3 i_d's PI controller design 65
5. SIMULATION RESULTS AND DISCUSSIONS 67
5.1 Simulation of the drive system 67
5.1.1 Simulink model of PMSM Drive system 67
5.1.2 The IQmath and DMC libraries 69

5.1.3 Software Organization 70
5.1.4 Simulation Results 71
5.1.5 Stability and Performance evaluation of the FL-PI Controller 79
5.2 DSP based controller....80
5.2.1 F2812 Device Simulator....81
5.2.2 Code Composer Studio 81
6. CONCLUSIONS AND RECOMMENDATIONS 83
6.1 Conclusions 83
6.2 Recommendations....85
APPENDIX A 89
APPENDIX B 89

LIST OF FIGURES

FIGURE **PAGE NUMBER**

Figure 2.1: Conventional Synchronous Motor [26] 8
Figure 2.2: Cross Sectional view of PMSM. 10
Figure 2.3: Rotor configurations studied: a) Surface Mounted PM (SPM); b) Interior PM (IPM) [33]. 13
Figure 2.4: Summary of Classification of AC Machines. 14
Figure 3.1: Separately excited DC Motor 18
Figure 3.2: Three-phase and two phase stator windings. 20
Figure 3.3: PMSM Dynamic stator q-axis and d-axis equivalent circuit. 23
Figure 3.4: PMSM equivalent circuits from steady state equations. 23
Figure 3.5: Motor axis. 26
Figure 3.6: Voltage decoupling. 29
Figure 4.1: Block Diagram of PMSM drive system. 31
Figure 4.2: Three Phase Inverter 34
Figure 4.3: Optical encoder [26]. 35
Figure 4.4: Output pulses of incremental encoder [25] 36
Figure 4.5: Single-phase inverter. 37
Figure 4.6: Sinusoidal Pulse width modulation. 37
Figure 4.7: Basic switching vectors, sectors and a reference vector. 41
Figure 4.8: Voltage space vector and its components in (abc axis) [23]. 42
Figure 4.9: Reference voltage as a combination of adjacent vectors in sector I [23] 44
Figure 4.10: Space Vector PWM switching patterns for the first two sectors. 45
Figure 4.11: Comparison SVPWM and Sinusoidal PWM. 47
Figure 4.12: Classical logic. 48
Figure 4.13: Fuzzy logic 48
Figure 4.14: General Structure of Fuzzy Logic Controller. 51
Figure 4.15: Fuzzy inferencing using Mamdani's max-min compositional operator. 53
Figure 4.16: Center of gravity defuzzification method. 54
Figure 4.17: PI control System 55
Figure 4.18: Structure of fuzzy logic based self tuning PI controller. 58
Figure 4.19: Member ship function of inputs (e, Δe). 59
Figure 4.20: Member ship functions of outputs (K_{P1}, K_{I1}). 59

Figure 4.21: Fuzzy inference block.....60
Figure 4.22: Variation of K_{p1} and $K_{I1}$with respect to error and change in error.....61
Figure 4.23: Block diagram of PMSM in q-axis.....62
Figure 4.24: Block diagram of q-axis Current loop. 63
Figure 4.25: A simplified i_q*'s* loop for PI design. 64
Figure 4.26: Block diagram of PMSM in d-axis.....65
Figure 4.27: The overall PMSM Control Structure. 66
Figure 5.1: Matlab/Simulink Model of the PMSM drive. 68
Figure 5.2: The Matlab/Simulink model of Fuzzy Logic-PI Speed Control structure. 68
Figure 5.3: The overall speed and current controller in Matlab/Simulink. 69
Figure 5.4: Flow chart of the system. 71
Figure 5.5: Speed response of the machine for 100rad/sec reference speed. 72
Figure 5.6: Developed electromagnetic torque for a step speed input. 73
Figure 5.7: i_a & i_b Currents as motor accelerating to 100 rad/sec speed input..... 73
Figure 5.8: Speed response of PI and FL-PI Controller for 100 rad/sec reference speed input..... 74
Figure 5.9: Reference speed and speed response at two step speed levels. 74
Figure 5.10: Reference speed and speed response for two ramp speed levels..... 75
Figure 5.11: Current drawn by the motor for two level speed commands. 75
Figure 5.12: Electromagnetic torque generated for the two level speed input. 76
Figure 5.13: Speed response when moment of inertia is increased by 50%. 76
Figure 5.14: Speed response when friction coefficient is increased by 50%..... 77
Figure 5.15: Speed response in load torque variation. 78
Figure 5.16: The Electromagnetic Torque generated and load torque. 78
Figure 5.17: Two of the three phase currents of the machine in load torque variation. 79
Figure 5.18: The FL-PI Controller Performance parameters..... 80
Figure 5.19: The relationship diagram of Matlab, CCS, and TI DSPs..... 82
Figure 5.20: Implementation model built using TI C2000 Toolbox. 82
Figure 5.21: a) The output control voltages V_{dref} and V_{qref} of the Controller in Simulink model. b) The output control voltages V_{dref} and V_{qref} of the Controller from the F2812 Device Simulator. 82

LIST OF TABLES

TABLE **PAGE NUMBER**

Table 4 1: Switching States of inverter phase leg a 34
Table 4.2: Switching vectors, phase voltages and output line to line voltages. 39
Table 4.3: Switching Time Calculation at Each Sector.....45
Table 4.4: Rule bases for determining the gains K_{P1} and K_{I1}. 60
Table 5.1: Performance Comparison of FL-PI and PI Controllers. **.....80**
Table B1: PMSM Motor Parameters.**.....89**

LIST OF ABBREVIATIONS AND SYMBOLS

AC/ac	alternating current
DC	direct current
rpm	revolution per minute
ADC	Analog-to-Digital Converter
CCS	Code Composer Studio
DSP	Digital Signal Processor
DMC	Digital Motor Control
FOC	Field Orient Control
IPM	Interior Permanent Magnet motor
mmf	magneto-motive force
MIPS	Millions of Instruction per second
PI	Proportional Integral
PM	Permanent Magnet
PMSM	Permanent Magnet Synchronous Machine
PWM	Pulse Width Modulation
QEP	Quadrature Encoder Pulse
Back-EMF	Back Electromagnetic Force
RTW	Real-Time Workshop
SPM	Surface-mounted Permanent Magnet motor
SVPWM	Space-Vector Pulse Width Modulation
VC	Vector Control
VSI	Voltage Source Inverter
* /ref	Reference quantity
d, q	synchronous reference frame quantities (d-axis, q-axis)
α, β	α-axis and β-axis stationary frame quantities
r	electrical quantity
m	mechanical quantity
Φ	Phase

ABSTRACT

This study is focused on the speed control performances of a Permanent Magnet Synchronous Motor (PMSM). Usually, a proportional-integral (PI) controller is used as a speed controller for a Permanent Magnet Synchronous Motor (PMSM) in high performance drive system despite the existence of many modern nonlinear control techniques. However, a PI controller is sensitive to speed changes, load disturbances and parameters variation without continuous tuning of its gains. The conventional approach to these issues is to tune the proportional and integral gains manually by observing the response of the system. The tuning of the PI parameters must be made on-line and automatic in order to avoid tedious tasks in manual control. The well-known Ziegler-Nichols method to tune the coefficients of a PI controller is very simple, but cannot guarantee to be always effective. For this reason, this thesis proposed the design of an on-line self tuning PI controller scheme using fuzzy logic controller (FLC). The performance of the proposed controller is tested through a wide range of reference speeds as well as with load variations through simulation using MATLAB/SIMULINK and Real Time Workshop (RTW) packages. The developed controller algorithm with field oriented control (FOC) is then simulated on a Texas Instruments TMS320F2812 Digital Signal Processor (DSP) device simulator. In this thesis work a FLC comprising 49 rules is proposed to improve the dynamic performance of the drive system. The simulation results show that the speed response of the proposed drive is unaffected by load torque & parameters variation. Furthermore, the developed controller works well even when the reference speed is changed to more complex trajectory, i.e., the developed controller speed regulation is unaffected by the nature of the reference speed trajectory. These shows remarkable performance improvement compared to conventional PI speed controller.

Keywords: PMSM, On-line self tuning PI Controller, Fuzzy Logic, MATLAB/SIMULINK, TMS320F2812 (DSP) device simulator.

CHAPTER ONE
INTRODUCTION

1.1Background Theory

The invention of modern permanent magnets (PM) with high energy density led to the development of dc machines with PM field excitation in 1950s. Introduction of PMs to replace the electromagnetic poles with windings requiring an electric energy supply source resulted in compact dc machines. Likewise in synchronous machines, the conventional electromagnetic field poles in the rotor are replaced by the PM poles and by doing so the slip rings and brush assembly are avoided. With the advent of high switching power transistor and silicon-controlled rectifier devices in the later part of 1950s, the replacement of the mechanical commutator with an electronic commutator in the form of an inverter was achieved. These two developments contributed to the development of PMSMs and brushless dc machines.

Permanent magnet synchronous motors (PMSM) are electrical motors that are widely used in motion-control applications in the low-to-medium power ratings such as robotics, house appliances, adjustable speed drives and electric vehicles. This popularity is justified by numerous advantages over commonly used motors. The absence of the external rotor excitation eliminates losses on the rotor, makes PMSM highly efficient and high torque to inertia ratio so that it gives fast response. In addition, the absence of the rotor winding renders slip rings on the rotor and brushes obsolete, and thus reduces the maintenance cost. The replacement of the rotor winding with PM in PMSM makes it compact structure or smaller in size that results a high power density. The heat loss in the rotor of PMSM that affects the machine operation is also negligible [1][2][26].

1.2 Motivation

In the recent years, demand for the use of permanent magnet synchronous motor drives has risen sharply in many industrial applications. This is partly because of the inherent advantages of these machines include high power density, low inertia, high efficiency, and high speed capabilities. Despite of the above all advantage, the PMSM is a coupled nonlinear

multivariable control structure which needs a complex nonlinear design. This makes the control performance of PMSM drives in various applications highly sensitive to variations of external load and system parameters [1] [7]. Since these variations are the dominant harmful factor in the PMSM drive system, high performance speed control against parameter variations and load disturbances takes on an added importance.

Conventionally vector controlled PMSM drive systems use a fixed gain proportional-integral (PI) controllers. However, the control performance of the PM synchronous motor servo drive is still influenced by uncertainties, which usually are composed of unpredictable plant parameter variations, external load disturbances, and unmodeled and nonlinear dynamics of the plant. Thus, the controller parameters must be adapted on-line continually. In the past decade many modern control theory (adaptive control techniques) have been developed to solve the problem such as model reference adaptive control (MRAC), Variable structure control (VSC), and self-tuning PI controllers. The design of all of the above controllers depends on the exact mathematical model of the drive system which is difficult to achieve practically.

Application of computational intelligence techniques like fuzzy logic control (FLC) can yield interesting solution in the field of speed control of drives. A Fuzzy logic control does not depend on the mathematical model of the drive system. In this thesis, a fuzzy logic based tuning of PI controller is proposed, which when included in the controller structure, ensures robustness against variations of some selected drive parameters.

This collaboration is practical as most of the industrial system that are using conventional PI controller can insert a FLC to their control system for optimization purposes without changing much of the system topology and scrapping the conventional controller [5].

1.3 Objective of the Study and Methodology

1.3.1 General Objective

This thesis is intended to study and design speed controller based on fuzzy logic, which is artificial intelligent technique, in conjunction with field oriented control (vector control)

technique for a permanent magnet synchronous motor (PMSM) drive. It is expected that this control scheme can track the reference speed well under parameter uncertainties and load torque disturbance.

1.3.2 Specific Objectives

Toward achieving the general objective mentioned**,** the following five specific objectives will be accomplished in this thesis:

- Studying the characteristics and modeling of the PMSM drive system
- Developing a Fuzzy Logic-PI speed control law based on the nonlinear model of the PMSM drive system.
- Simulating the speed control and load torque tracking of the PMSM motor using vector control realized by space vector which have been done on MATLAB/SIMULINK
- Generating a C-code for the SIMULINK model via real time workshop feature of MATLAB
- Simulating the generated code on the DSP device simulator using PIL

1.3.3 Methodology

The methodology of this thesis involves the following tasks for each specific objective. The first task is the literature reviews where all the theoretical information regarding the PMSM drive is gathered and a comparison of previous similar research is studied. This is followed by studying the characteristics and modeling of PM motor drive theory. Based on the nonlinear dynamic model of the PMSM drive, a Fuzzy Logic tuning PI control law is developed. Hereafter, simulation of speed control and load torque tracking of the motor using vector control is realized by space vector method which has been done on MATLAB/Simulink. Later on in this thesis, a fixed point simulink model of the overall system is created in order to simulate the algorithm on F2812 DSP device simulator, which is available in simulink library. The c-code has been generated from the fixed point model via Real time workshop of MATLAB module. After being sure the generated code is efficient and optimized, it is tested using F2812 DSP device simulator in order to verify the controller algorithm works or not.

1.4 Literature review

Speed control of PM (permanent magnet) motor drives has been a topic of interest for the last twenty years. And different papers have been published reporting different controller design for such drives.

In 2008 Mutasim Nour, Omrane Bouketir & Ch'ng Eng Yong [5] presented a Self-Tuning of PI Speed Controller Gains Using Fuzzy Logic Controller for PMSM as test bed to adapt the controller gains to speed changes, load disturbances and parameters variations. Hence, an on-line self-tuning scheme using fuzzy logic controller (FLC) is proposed in this paper. The performance of the developed proposed controller is tested through a wide range of speeds as well as with load and parameters variations through simulation using MATLAB/SIMULINK. The simulation results show that the developed controller can well adapt to speed changes as well as sudden speed reduction besides fast recovery from load torque and parameters variation and these show improvement compared to conventional PI controller performance. In this Paper the controller scheme needs tuning of the input/output scaling factors which is additional job for the processor which increases the time of response of the system.

In 2007 Yanpeng Dou, Zhang Ze [6] discussed Design and realization of fuzzy self-tuning PID speed controller based on TMS320F2812 DSPs to apply fuzzy self-tuning PID controller to AC-speed adjustable system, and special attention is given on how to realize this controller using fuzzy search table method in C++ language based on TMS320F2812, which is the newest 32-bit fixed point DSP. And the results show that the controller improves both the dynamic characteristics and static characteristics of drive system. The paper only compares the speed response of the proposed controller and PID controller without any load torque and parameter variation.

In 2007 Limei Wang, Mingxiu Tian and Yanping Gao [8] reviewed Fuzzy Self-adapting PID Control of PMSM Servo System to adjust PID parameters adaptively on-line using fuzzy inference method for the varying state of the system. Because the traditional self adapting control is very difficult to realize, which need on-line identification of the system parameters and the real-time change of control strategy. The proposed control scheme was verified by

simulation using MATLAB and shows better performance than conventional PID controller in the PMSM drive system. This paper compares only the speed responses of the proposed controller and PID controller for step input reference speed without considering any other speed trajectories, load disturbances, and parameter variations.

In 2006 Rajesh Kumar, R. A. Gupta, and Bhim Singh [7] presented a critical analysis of intelligent tuned PID controllers for the Permanent Magnet Synchronous Motor drive so that PID control strategies, based on fuzzy logic, neural network and genetic algorithms are reviewed. Different tuning algorithms and their effect on dynamic performance of PMSM drive in the real time frame are illustrated in terms of starting and speed reversal time, steady state error in speed, overshoot, performance parameters and speed and torque ripple. Good agreements between different methods has been observed and presented.

A fuzzy-logic-based speed control of vector Controlled Permanent Magnet Synchronous Motor can also be designed that completely replaces the traditional PI controller. The fuzzy-logic controller (FLC) is more robust and, hence, found to be a suitable replacement of the PI controller for the high performance drive systems. But this controller needs a highly experienced operator to design it and the control system is completely replaced which is still additional cost for the PMSM drive in industrial systems [20].

A composite control of fuzzy and PI or fuzzy and PID is also possible for Permanent Magnet Synchronous Motor (PMSM) drives to achieve fast dynamic response and minimum steady state error. A switching algorithm is created to switch between fuzzy control and PI(PID) control and results showed that the controller had a quick dynamic response, and eliminated basic steady-state error, dynamic characteristics and stability. Using this composite control of fuzzy and PI for PMSM drive in Industrial processes cause changing of the overall system topology which increases the cost of optimization of the control system[21][22].

A number of other papers also present advantages of Fuzzy-logic based controller techniques over PI and verified to implement sensored and sensorless control of PMSM in normal and field weakening region.

1.5 Thesis Organization

The thesis is organized into six chapters including this introduction. The rest of the thesis is organized as follows:

Chapter II describes the theory and operation principle of PMSM. Different PMSM construction details, difference with synchronous motors, starting characteristics of PMSM, and its different applications are presented.

Chapter III In this chapter a dynamic modeling of the PMSM drive with Field oriented control based on co-ordinate transformation is described.

Chapter IV This chapter has two main parts. The first one deals with the description of drive system of PMSM which includes different components such as Permanent Magnet Synchronous Motor, position & speed sensor, current sensor, Controller, inverter & power switches, and space vector PWM modulation algorithm. The second part explained how Fuzzy logic-PI controller is designed a step by step for surface mounted permanent magnet synchronous motor and the control scheme is shown here.

Chapter V This chapter discusses on simulation of the drive system on MATLAB/Simulink including simulation result and explains the simulation of the generated code with digital signal processor device simulator to verify the controller algorithm. Included in this chapter, simulation results based on load torque disturbance and motor parameter variation is depicted.

Finally, **Chapter VI** draws the conclusions from the work done in this thesis and recommends further research possible in the future.

CHAPTER TWO

PMSM AND ITS PRINCIPLE OF OPERATION

Permanent Magnet Machines are electromechanical devices using magnets to produce a magnetic flux in the air gap. There are two major classifications of ac motors. The first one is induction motors that are electrically connected to power source through electromagnetic coupling, the rotor and the stator fields interact, creating rotation without any other power source .The second is synchronous motors that have fixed stator windings that are electrically connected to the ac supply with a separate source of excitation connected to field windings when the motor is operating at synchronous speed.

Among the synchronous motor types the permanent magnet synchronous motor (PMSM) is one possible design of three phase synchronous machines. The stator of a PMSM has conventional three phase windings. In the rotor, PM materials have the same function of the field winding in a conventional synchronous machine. Their development was possible by the introduction of new magnetic materials, like the rare earth materials. The use of a PM to generate substantial air gap magnetic flux makes it possible to design highly efficient PM motors [1][2][32].

2.1 Introduction to Synchronous Motor

Synchronous Motor has the characteristic of constant speed between no load and full load. They are capable of correcting the low power factor of an inductive load by adjusting the excitation system.

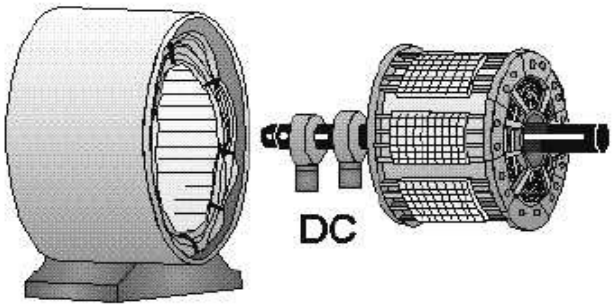

Figure 2.1: Conventional Synchronous Motor [26]

To understand the principle of operation of Synchronous Motor, assume that the application of three phase ac power to the stator causes a rotating magnetic field to be set up around the rotor. The rotor is energized with dc excitation (it acts like a bar magnet). The strong rotating magnetic field attracts the rotor field activated by the dc excitation if only rotor is running near to synchronous speed by some means. The interaction between the two magnetic fields results in a strong turning force on the rotor shaft. The rotor is therefore able to turn a load as it rotates at the same speed with the rotating magnetic field. However, one of the drawbacks of a synchronous motor is that it cannot be started from a standstill by applying three-phase ac power to the stator winding. When AC power is applied to the stator, a rotating magnetic field at a speed of the angular frequency of stator current appears immediately. This rotating field rushes past the rotor poles quickly. But rotor does not have a chance to get started due to inertia. In effect, the rotor is repelled first in one direction and then the other. Hence, synchronous motor in its purest form has no starting torque. It has torque only when it is running at synchronous speed [26].

For the motor to operate, the rotor should first reach a synchronous speed. This can be done in three ways: by driving the rotor to the synchronous speed (with an external machine), by starting the rotor (which has to be equipped with a starting cage) as in induction motors, or by supplying the stator winding with variable frequency, beginning from zero to the rated frequency. The latter method can be used if the winding is supplied from a frequency converter.

A Synchronous Machine is an AC Machine whose speed under steady state condition is proportional to the frequency of the current in the stator. The magnetic field created by the

stator currents rotates at the same speed as that created by field current on the rotor (which is rotating at synchronous speed). The synchronous speed, Ns, is determined by the frequency of the stator supply, *fs* and the number of stator poles. Unlike Induction Motor, Synchronous Motor is excited by a separate DC or permanent magnet source. The stator of the three-phase synchronous motor normally has a sine distributed three-phase winding. The synchronous speed is given by the equation (2.1).

$$N_s = \frac{60\, f_s}{P} \tag{2.1}$$

where

fs - frequency of ac supply, P - Number of pole pairs, and N_s - Synchronous speed.

From the above equation, speed of Synchronous Motor totally depends on the supply frequency. Therefore, synchronous speed is controlled by varying the supply frequency.

2.2 Permanent Magnet Synchronous Motor

A Permanent Magnet Synchronous Motor (PMSM) is a synchronous motor that uses permanent magnets to produce the air gap magnetic field rather than using electromagnets. It has a multiphase stator and the stator electrical frequency is directly proportional to the rotor speed in the steady state. However, it differs from a traditional synchronous machine in that it has permanent magnets in place of the field winding and otherwise has no rotor conductors. The use of permanent magnets in the rotor enhances efficiency, eliminates the need for slip rings, and eliminates the electrical rotor dynamics that complicate control (particularly vector control). The combination of an inner permanent magnet rotor and outer windings offers the advantages of low rotor inertia, efficient heat dissipation, and reduction of the motor size.

The PMSMs involve adjustment of the stator supply frequency, proportionally as the rotor speed is varied, so that the stator field always moves at the same speed as the rotor. The rotating magnetic fields of the stator (armature) and the rotor (excitation) system are then always in synchronous motion producing a steady torque at all operating speeds. This is analogous to the D.C motor in which the armature and excitation fields are synchronous but stationary for all operating speeds. PMSM requires the very accurate measurement of rotor

speed and position and the very precise adjustment of the stator frequency. Rotor position sensing is done by an encoder, resolver… etc which forms part of a control loop of an adjustable frequency inverter feeding the stator winding.

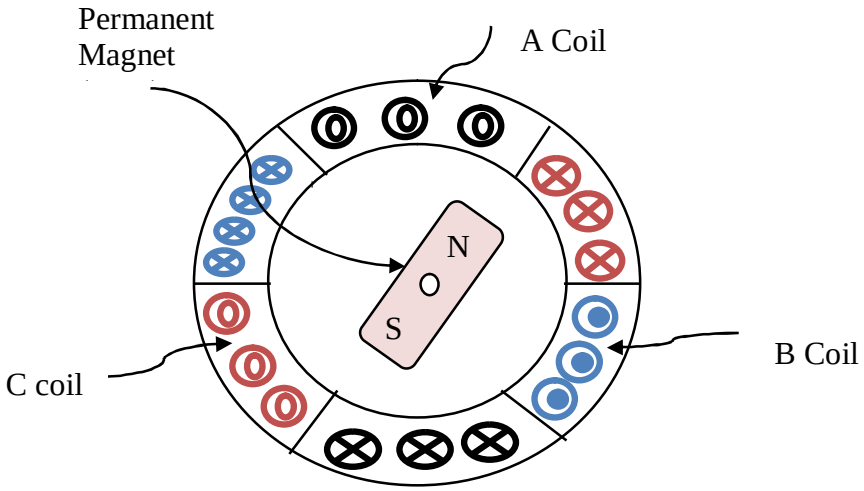

Figure 2.2: Cross Sectional view of PMSM.

2.2.1 Permanent Magnet Materials

Materials to retain magnetism were introduced in electrical machine research in the 1950s. There has been a rapid progress in these kinds of materials since then. The properties of the permanent magnet material affect directly the performance of the motor and proper knowledge is required for the selection of the materials and for understanding PM motors. The materials such as alnico-5, ferrites (ceramics), samarium-cobalt, and neodymium boron iron are available as PMs for use in machines. The particular choice of magnets and other design factors is important, but does not directly influence the basic principles of power converter control [1].

2.2.2 Classification of Permanent Magnet Motors

2.2.2.1 Magnetization of PMs

PMs are magnetized with certain orientation or direction such as radial, parallel, or any other direction. The magnetization orientation strongly influences the quality of the air gap flux

density distribution and indirectly affects the power density in a given arrangement of the machine with PMs. Radial and parallel magnetization orientation are prevalent in practice whereas other forms of magnetization are yet to make their presence felt even when they have been known to possess unique advantages in some cases.

PM motors can be classified by the magnetization orientation of PMs as *radial* magnetization and *parallel* magnetization. The radial magnetization is along the radius of rotor while the parallel magnetization is parallel to the edges of rotor.

2.2.2.2 Direction of Field Flux

The PMSM can be broadly classified on the basis of the direction of field flux as follows:

1. Radial field: The flux direction is along the radius of the machine.
2. Axial field: The flux direction is parallel to the rotor shaft.

The radial field PM machines are common whereas the axial field machines are coming into prominence in a small number of applications due to their higher power density and have become a topic of interest for study. The field flux is along the radius of the motor in radial magnetization and is perpendicular to the radius of the motor in parallel magnetization.

2.2.2.3 Flux Density Distribution

PM motors are classified on the basis of the flux density distribution and the shape of current excitation. They are PMSM and PM brushless motors (BLDC). The PMSM has a sinusoidal-shaped back EMF (it is an induced voltage in the stator by the motion of the rotor) and is designed to develop sinusoidal back EMF waveforms. Generally the PMSM has a:

- Sinusoidal distribution of magnet flux in the air gap
- Sinusoidal current waveforms, and
- Sinusoidal distribution of stator conductors.

BLDC has a trapezoidal-shaped back EMF and is designed to develop trapezoidal back EMF waveforms. It has:

- Rectangular distribution of magnet flux in the air gap
- Rectangular current waveform
- Concentrated stator windings

2.2.2.4 Permanent Magnet Radial Field Motors

In PMSMs, the magnets can be placed in different ways on the rotor. Depending on the placement they are called either as Surface Permanent Magnet Motor *(SPM)* or Interior Permanent Magnet *(IPM)* Synchronous Motor.

Surface mounted PM motors have a surface mounted permanent magnet rotor. Each of the PM is mounted on the surface of the outer periphery of rotor laminations. This arrangement provides the highest air gap flux density as it directly faces the air gap without the interruption of any other medium such as part of rotor laminations. Drawbacks of such an arrangement are lower structural integrity and mechanical robustness as they are not tightly fitted into the rotor laminations to their entire thickness. This configuration is used for low speed applications because of the limitation that the magnets will fly apart during high-speed operations. These motors are considered to have small saliency, thus having practically equal inductances in both quadrature and direct axes. For a surface permanent magnet motor, $L_d = L_q$. Figure 2.3 shows the placement of the magnet.

Interior PM Motors have interior mounted permanent magnet rotor. Each permanent magnet is mounted inside the rotor. The interior PM rotor construction is mechanically robust and therefore suited for high-speed applications. The manufacturing of this arrangement is more complex than the surface mount. It is not as common as the surface mounted PM type. By designing a rotor magnetic circuit such that the inductance varies as a function of rotor angle, the reluctance torque can be produced in addition to the mutual reaction torque of synchronous motors. These motors are considered to have saliency with q axis inductance (L_q) greater than the d axis inductance (L_d) ($L_q > L_d$). In this thesis SPM radial flux machine with classical winding and lamination has been chosen due to the following reasons:

- The SPM drive without reluctance torque is simpler to analyze and design than an IPM drive.
- The topology of a radial flux machine with classical winding and lamination has been chosen because of the well-known and established technology.

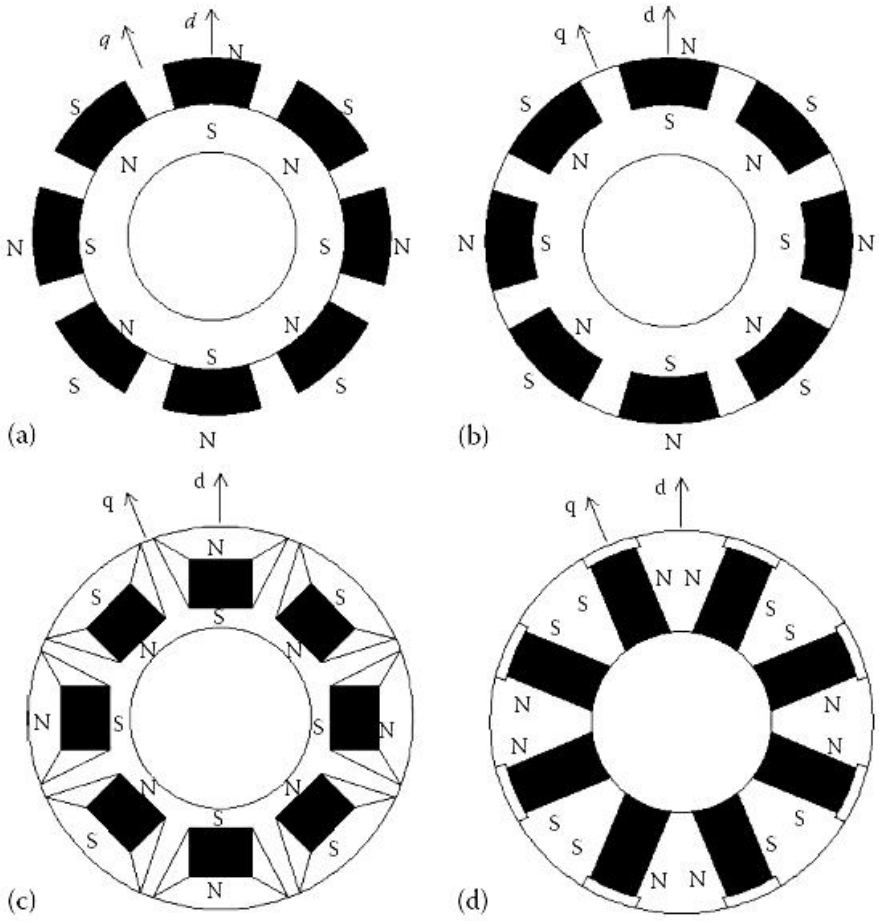

(a) (b)

Figure 2.3: Rotor configurations studied: (a) Surface PM (SPM) synchronous machine. (b) Surface inset PM (SIPM) synchronous machine. (c) Interior PM (IPM) synchronous machine. (d) Interior PM synchronous machine with circumferential orientation [1].

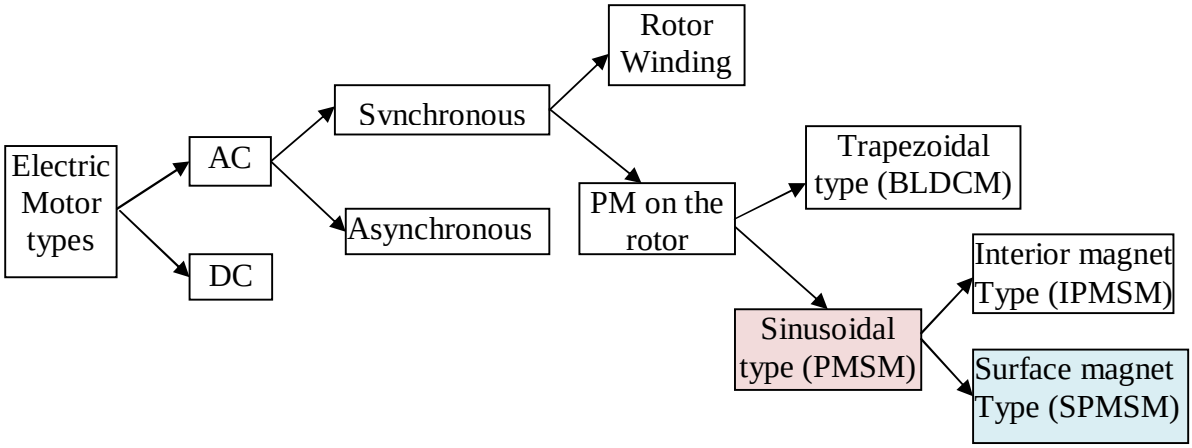

Figure 2.4: Summary of Classification of AC Machines.

2.3 Starting Characteristics of PMSM

PMSMs can neither start nor run simply by applying AC power to the stator winding without special attention because the net torque on the rotor is zero unless the rotor winding is rotating at nearly synchronous speed with appropriate excitation applied to the moving winding. For this reason, various arrangements have been created for starting PMSM. Starting from unknown rotor position may be accompanied by a temporary reverse rotation or may cause a starting failure. These eventualities are not tolerable in many applications. Thus, when the initial rotor position information is not available proper starting procedure must be implemented for safe startup. According to the various proposals in literature the possible starting procedures can be grouped with reference to the basic principle as follows:

- ❖ starting from predetermined rotor position established by proper feeding;
- ❖ open-loop startup (V/f);
- ❖ estimation of the rotor position at standstill by means of specific algorithms

The first method refers to the possibility of aligning the rotor magnet axis in the direction of a stator magnetic field .This can be accomplish through closed loop current control (i.e. by the proper setting of the position feedback in a field oriented controller, or in an open loop

scheme, simply imposing a specific inverter gate pattern to align with one of the phase axes. The reliability of this method is affected by the presence of the load torque, whose value can cause a displacement between the imposed alignment position and the actual one.

The open loop startup is intended as the acceleration of the motor following a rotating stator field whose angular position is generated in an open-loop scheme. This method is usually adopted in back-EMF-based sensorless scheme, and the open-loop operation is maintained until a given speed at which the rotor position estimate is sufficiently accurate. The critical point of this method is the choice of the time variation law of the open loop position. It must be carefully selected in order to assure a safe starting with minimum oscillation up to the maximum torque.

Among the specific algorithms for rotor position estimation at standstill, an interesting approach is the use of a field oriented control scheme with incremental optical encoder used to measure the rotor position.

2.4 Why concentrate this study on PMSM?

The significant advantages of PMSM attracting researchers and industries make it highly competitor to other motors like Induction Motors & DC Motors.

PMSMs have many advantages. To mention some;

- They have high torque to inertia (lower weight). That is better dynamic performance than conventional one.
- High power density.
- High efficiency (That is no current in the rotor means no copper loss) and reliability.
- Avoidance of brushes and slip rings makes the machine less audible noise, longer life, sparkless (no fire hazard) and is used for high speed applications.
- Efficient heat dissipation.

Even though PM machines have aforementioned merits, they have the following demerits:

- They have complex control.
- There is a possibility of demagnetization of the rotor magnet.
- If demagnetization occurs, there will be a reduction of torque production.

- There is a problem of maintenance of rotor magnet.

2.5 Applications

Among many applications of PM synchronous motor, here are the following:

Robotics and factory automation (servo drives)

- pick and place robots (Motion control)
- positioning tablets
- automatic guided vehicle

Computer and office equipment

- copier and microfilm machines
- printers/plotters
- tape drivers

Appliances

- washers
- blowers
- compressors
- heating
- Ventilation and air conditioning

  etc.

CHAPTER THREE
DYNAMIC MODELING OF PMSM DRIVE

Although traditional per-phase equivalent circuits have been widely used in steady-state analysis and design of AC machines, it is not appropriate to predict the dynamic performance of the motor. In order to understand and analyze vector control of AC motor drives, a dynamic model is necessary. As the application of AC machines has continued to increase over this century, new techniques have been developed to aid in their analysis. The significant breakthrough in the analysis of three-phase machines was the development of the reference frame theory. Using these techniques, it is possible to transform the machine model to another reference frame. By careful choice of the reference frame, it proves possible to simplify vastly the complexity of the mathematical machine model. While these techniques were initially developed for the analysis and simulation of AC machines, they are now important tools in the digital control of such machines [1].

3.1 Field Oriented Control (FOC)

The principle of vector control (FOC) of electrical drives is based on the control of both the magnitude and the phase of each phase stator current and voltage. This control is based on projections which transform a three phase time and speed dependent system into a two co-ordinate (d and q) time invariant system. These projections lead to a structure similar to that of a DC machine control. In order for the PMSM to behave like DC motor, the control needs knowledge of the position of the instantaneous rotor flux or rotor position. The idea of Field Oriented Control method is to control the current of the machine in space quadrature with the magnetic flux created by the permanent magnets as in the case of DC motors [2] [23].

A DC Motor consists of a field structure utilizing a stationary dc excited winding or permanent magnets and a rotating armature winding supplied through a commutator and brushes. The action of the commutator is to reverse the direction of the armature winding currents as the coils pass the brush position that the armature current distribution is fixed in space no matter what rotor speed exists. The field flux and armature mmf are maintained in a mutually perpendicular orientation independent of rotor speed. The result of this

orthogonality is that the field flux is unaffected by the armature current. I.e. the field flux and the armature mmf are decoupled [18].

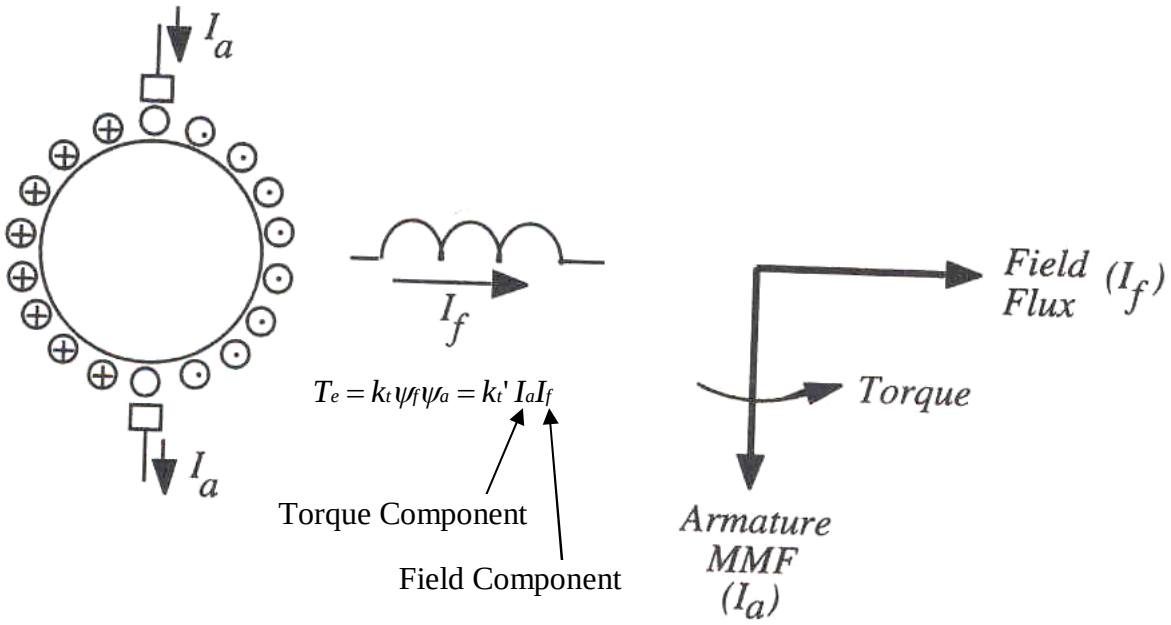

Figure 3.1: Separately excited DC Motor [26].

Like separately excited DC motor Field Oriented Control seeks to recreate these orthogonal components in AC machines in order to control the torque producing current separately from the magnetic flux producing current so as to achieve the responsiveness of a DC motor.

Field oriented control structure handles instantaneous electrical quantities. This makes the control accurate in every working operation (steady state & transient) and independent of the limited bandwidth mathematical model. Field oriented controlled machines need two constants as input references: the torque component (aligned with the q-coordinate) and the flux component (aligned with d- coordinate). The FOC thus solves the classic scheme problems, in the following ways [26]:

- The ease of reaching constant reference (torque component and flux component of the stator current)

- The ease of applying direct electromagnetic torque, T_{em} control in the (d, q) reference frame. $T_{em} = \frac{3}{2} P \psi_m i_q$

By maintaining the amplitude of the rotor flux (ψ_m) at a fixed value we have a linear relationship between torque and torque component (i_q). We can then control the torque by controlling the torque component of stator current vector.

3.2 Reference frame Transformation (3-Φ to 2-Φ Transformations)

Vector control reconstructs orthogonal components of the stator current in AC machine as torque producing current and magnetic flux producing current. In order to create the perpendicular components of the stator current of PMSM which is in the form of a vector, concept of coordinate transformation is required Assume that the three phase supply voltage is balanced. The Clarke and Parke transformation is a transformation of coordinates from the three phase stationary coordinate system to the dq rotating coordinate system.

A dynamic model for the three-phase PMSM can be derived from the two phase machine if the equivalence between the three and two phases is established. The equivalence is based on the equality of the mmf produced in the two-phase and three-phase windings and on equal current magnitudes. Assuming that each of the three-phase windings has *N* turns per phase, and equal current magnitudes, the two-phase windings will have $3/2\,N$ turns per phase for mmf equality [1].

The transformations are usually based on following assumptions:

- Space harmonics of the flux linkage distribution are neglected.
- Rotor flux is assumed to be concentrated across d-axis and zero flux along q-axis
- Slot harmonics and deep bar effects are not considered
- Rotor flux is assumed to be fixed at a given operating point
- Machine core losses are negligible
- Saturation is neglected.

- Rotor temperature alters the flux, but the variation with time is assumed to be negligible
- Permanent magnets behave linearly.
- Neutral point is isolated.
- There are no field current dynamics

Rotor reference frame is chosen because rotor position determines independently the stator voltages & currents, induced emfs, and torque. The d-q coordinate system rotates at the same speed of rotor; there is zero speed difference between rotor speed and revolving stator field. The stator d-q axis has a fixed phase relationship with rotor magnetic axis which is d-axis in modeling.

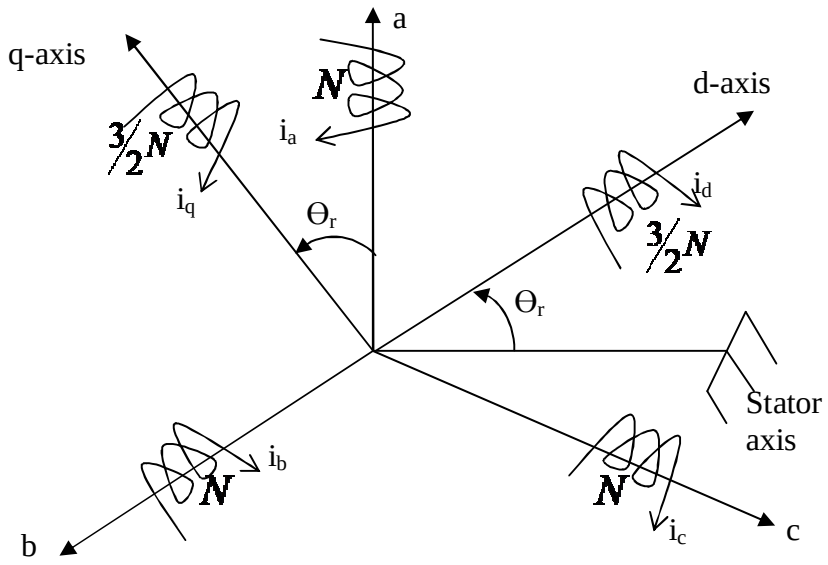

Figure 3.2: Three-phase and two phase stator windings.

Let the magnetomotive force mmf=f=NI

$$f_q = \frac{3}{2} N i_q = \cos\theta_r i_a N + \cos(\theta_r - \frac{2\pi}{3}) i_b N + \cos(\theta_r + \frac{2\pi}{3}) i_c N$$
$$f_d = \frac{3}{2} N i_d = \sin\theta_r i_a N + \sin(\theta_r - \frac{2\pi}{3}) i_b N + \sin(\theta_r + \frac{2\pi}{3}) i_c N \quad (3.1)$$

Removing N from both sides results a matrix equation to determine the d & q stator current components in the rotor reference frame directly from i_a, i_b, & i_c in the stationary reference frame.

$$\begin{bmatrix} i_q \\ i_d \end{bmatrix} = \frac{2}{3} \begin{bmatrix} \cos\theta_r & \cos(\theta r - 2\pi/3) & \cos(\theta_r + 2\pi/3) \\ \sin\theta r & \sin(\theta_r - 2\pi/3) & \sin(\theta_r + 2\pi/3) \end{bmatrix} \begin{bmatrix} i_a \\ i_b \\ i_c \end{bmatrix} \quad (3.2)$$

$$i_{qd} = [T_{abc}] i_{abc} \quad (3.3)$$

where

$$i_{qd} = \begin{bmatrix} i_q & i_d \end{bmatrix} \quad (3.4)$$

$$i_{abc} = \begin{bmatrix} i_a & i_b & i_c \end{bmatrix}^t \quad (3.5)$$

$$T_{abc} = \frac{2}{3} \begin{bmatrix} \cos\theta_r & \cos(\theta_r - 2\pi/3) & \cos(\theta_r + 2\pi/3 \\ \sin\theta_r & \sin(\theta_r - 2\pi/3) & \sin(\theta_r + 2\pi/3) \end{bmatrix} \quad (3.6)$$

The transformation from the two-phase stator currents in rotor reference frame to three-phase stator currents in stationary reference frame can be obtained as in equation (3.7).

$$i_{abc} = [T_{abc}]^{-1} i_{qd} \quad (3.7)$$

where

$$[T_{abc}]^{-1} = \begin{bmatrix} \cos\theta_r & \sin\theta_r \\ \cos(\theta_r - 2\pi/3) & \sin(\theta_r - 2\pi/3) \\ \cos(\theta_r + 2\pi/3 & \sin(\theta_r + 2\pi/3) \end{bmatrix} \quad (3.8)$$

As we can see from the equations (3.2) and (3.8), the coordinate transformations from the stationary reference frame to rotating reference frame and vice versa needs an accurate rotor flux position θ_r.

3.3 Modeling of PMSM

PMSM is very similar to the standard wound rotor synchronous machine except that the PMSM has no damper windings and excitation is provided by a permanent magnet instead of a field winding. Hence the *d, q* model of the PMSM can be derived from the well-known model of the synchronous machine with the equations of the damper windings and field current dynamics removed [1] [2].

3.3.1 Voltage Equation

Here is the derivation of the electrical equations which are greatly simplified due to the concept of rotating transformation. The two axis voltage equations for the stator winding which are of an IPMSM (but is the same for SPMSM where L_d and L_q have the same value) are given by equations:

$$\begin{aligned} V_q &= R_s i_q + \frac{d}{dt}(\psi_q) + \omega_r \psi_d \\ V_d &= R_s i_d + \frac{d}{dt}(\psi_d) - \omega_r \psi_q \end{aligned} \tag{3.9}$$

where

$$\begin{aligned} \psi_d &= L_d i_d + \psi_m \\ \psi_q &= L_q i_q \end{aligned} \tag{3.10}$$

V_d & V_q are the (d,q) axis stator voltages

i_d & i_q are the (d,q) axis stator currents

L_d & L_q are the (d,q) axis inductances

θ_r is rotor electrical position

ω_r is rotor electrical angular velocity

ψ_m is flux linkage due to the rotor magnets linking the stator

ψ_d & ψ_q are the (d,q) axis stator flux linkages

R_s is stator winding resistance

Substituting the equations (3.10) in to (3.9) the dynamic equation gives a more convenient equation for equation (3.11)

$$V_q = (R_s + L_q \frac{d}{dt}) i_q + \omega_r L_d i_d + \omega_r \psi_m$$
$$V_d = (R_s + L_d \frac{d}{dt}) i_d - \omega_r L_q i_q \quad (3.11)$$

3.3.2 Equivalent Circuits

From the dynamic equation (3.11) the equivalent circuit of the PMSM can be derived for the stator q-axis and d-axis coordinates. During steady state operation, the *d-q* axis currents are constant quantities. Hence the dynamic equivalent circuit can be reduced to the steady state circuit shown in Figure 3.3 and 3.4.

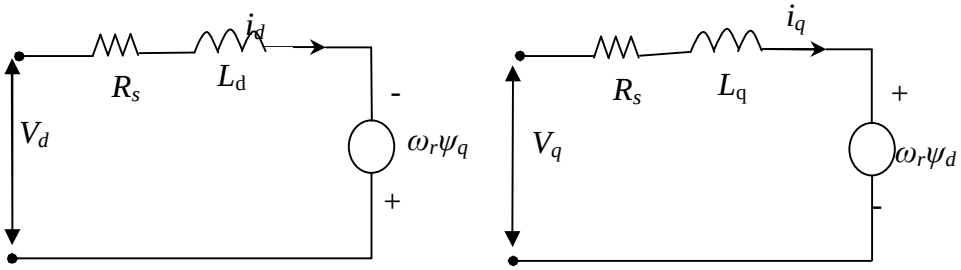

Figure 3.3: PMSM Dynamic stator q-axis and d-axis equivalent circuit.

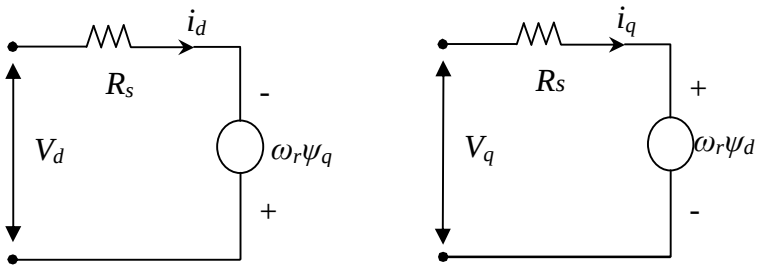

Figure 3.4: PMSM equivalent circuits from steady state equations.

3.3.3 Power Equivalence

The power input to the three-phase machine has to be equal to the power input of the two phase machine to have meaningful interpretation in the modeling, analysis, and simulation.

Such an identity is derived in this section. The three-phase instantaneous power input is given by:

$$P_{in} = V^{t}_{abc} i_{abc} = [V_a \quad V_b \quad V_c] \begin{bmatrix} i_a \\ i_b \\ i_c \end{bmatrix} \tag{3.12}$$

$$P_{in} = V_a i_a + V_b i_b + V_c i_c \tag{3.13}$$

Using equation (3.7) the inverse transformation from two phase rotating reference frame to three phase stationary reference frame for voltage components is given as equation (3.14).

$$V_{abc} = \left[T_{abc}\right]^{-1} V_{qd} \tag{3.14}$$

Substituting equation (3.14) to (3.13) results:

$$Pi_n = \left(\left[T_{abc}\right]^{-1} V_{qd}\right)^{t} \left[T_{abc}\right]^{-1} i_{qd} \tag{3.15}$$

$$P_{in} = \frac{3}{2}\left[V_q i_q + V_d i_d\right] \tag{3.16}$$

Input power remains constant for all reference frames.

3.3.4 Electromagnetic Torque Equation

The electromagnetic torque is the most important output variable that determines the mechanical dynamics of the machine such as the rotor position and speed. Therefore, its importance cannot be overstated in all the simulation studies. It is derived from the machine matrix equation by looking at the input power and its various components such as resistive losses, mechanical power, and the rate of change of stored magnetic energy. Elementary reasoning leads to the fact that there cannot be a power component due to the introduction of reference frames. Similarly, the rate of change of stored magnetic energy could only be zero in steady state. Hence, the output power is the difference between the input power and the resistive losses in a steady state. Note that dynamically, the rate of change of stored magnetic energy need not be zero. Based on these observations, the derivation of the electromagnetic torque is made as follows [1] [17] [28].

Substituting equation (3.9) to the power equation (3.16) gives:

$$P_{in} = \frac{3}{2}(R_s i_d{}^2 + R_s i_q{}^2) + \frac{3}{2}(i_d \frac{d}{dt}\psi_d + i_q \frac{d}{dt}\psi_q) + \frac{3}{2}\omega_r(\psi_d i_q - \psi_q i_d) \quad (3.17)$$

The first term of the above equation is the power loss in the conductors, the second term is the time rate of change of stored energy in the magnetic fields and the third term is the energy conversion from electrical to mechanical energy. The torque can be derived from the third term of the power equation and written as:

$$P_m = \omega_m T_{em} = \frac{3}{2}\omega_r(\psi_d i_q - \psi_q i_d) \quad (3.18)$$

where

P_m is output mechanical power

ω_m is mechanical angular velocity of the rotor shaft

T_{em} is generated electromagnetic torque

The mechanical speed is related to electrical speed by

$$\omega_r = \omega_m P \quad (3.19)$$

where

P is number of pole pairs

Substituting equation (3.19) to (3.18) results:

$$T_{em} = \frac{3}{2}P(\psi_d i_q - \psi_q i_d) \quad (3.20)$$

Hereafter substituting the equation (3.10) in to equation (3.20) the torque equation can also be expressed in the following way and equated to the mechanical equation (3.21).

$$T_{em} = \frac{3}{2}P[\psi_m i_q + (L_d - L_q) i_q i_d]$$

$$= T_L + J\frac{d}{dt}\omega_m + B\omega_m \quad (3.21)$$

The first term is called “mutual reaction torque” occurring between i_q and the permanent magnet, while the second term corresponds to “reluctance torque” due to the difference in d-axis and q-axis reluctance (or inductance). The motor used in this thesis is surface mounted PMSM which means that $L_d = L_q$, due to the same reluctance paths in rotor d and q-axis, and therefore the “reluctance torque” is equal to zero, so the torque expression for SPMSM is:

$$T_{em} = \frac{3}{2} P \psi_m i_q \tag{3.22}$$

Since the number of pole pairs and the magnetic flux linkages are constant, then the torque is directly proportional to q-axis current i_q.

$$T_{em} = K_t i_q \tag{3.23}$$

Where $K_t = {}^{3}\!/_{2}\, P \psi_m$ is called torque constant.

The torque equation (3.23) is now similar to that in a separately excited DC motor, where i_q corresponds to the armature current of the DC machine and torque can be controlled by controlling i_q. Constant torque control strategy is derived from field oriented control, where the maximum possible torque is desired at all times like the dc motor. This is performed by making the torque producing current i_q equal to the supply current I_s. This is achieved by controlling i_d to be equal to zero [1].

3.3.5 Steady State Torque Characteristics of SPMSM

To analyze the steady state torque characteristics of SPMSM, consider a set of balanced three phase currents as input to the stator windings.

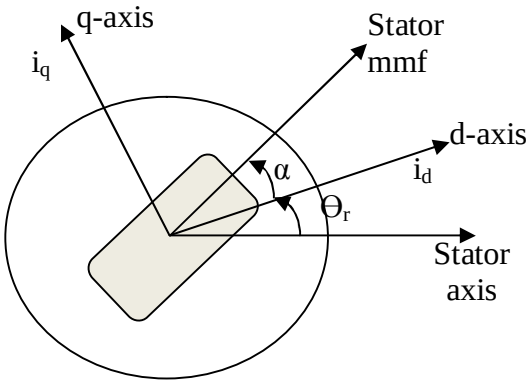

Figure 3.5: Motor axis.

$$\begin{aligned} i_a &= \mathrm{I_m} \sin(\omega_r t + \alpha) \\ i_b &= \mathrm{I_m} \sin(\omega_r t + \alpha - {}^{2\pi}\!/_{3}) \\ i_c &= \mathrm{I_m} \sin(\omega_r t + \alpha + {}^{2\pi}\!/_{3}) \end{aligned} \tag{3.24}$$

$$\begin{bmatrix} i_a \\ i_b \\ i_c \end{bmatrix} = \begin{bmatrix} \sin(\omega_r t + \alpha) \\ \sin(\omega_r t + \alpha - 2\pi/3) \\ \sin(\omega_r t + \alpha + 2\pi/3) \end{bmatrix} [\mathrm{I_m}] \tag{3.25}$$

Substituting equation (3.25) to equation (3.2) gives

$$\begin{bmatrix} i_q \\ i_d \end{bmatrix} = \mathrm{I_m} \begin{bmatrix} \sin\alpha \\ \cos\alpha \end{bmatrix} \tag{3.26}$$

i.e.

$$i_q = \mathrm{I_m} \sin\alpha \tag{3.27}$$

$$i_d = \mathrm{I_m} \cos\alpha \tag{3.28}$$

Inserting equation (3.27) and (3.28) in to equation (3.22) gives:

$$T_{em} = 3/2\, P[\psi_m \mathrm{I_m} \sin\alpha) \tag{3.29}$$

where

α is termed the torque angle (the angle between the rotor field and stator mmf) as it directly influences the air gap torque.

$\mathrm{I_m}$ is the magnitude of the stator current phasor and ω_r is the rotor electrical speed.

Key results:

1) Control of phase (α, torque angle) and magnitude of stator current phaser is achieved through the inverter determines the torque and its control.

2) Control of the angular frequency of the stator current phaser determines rotor electrical speed ω_r rad/s.

3.3.6 Voltage Decoupling Control

To achieve completely independent control of the direct-axis stator current i_d (field producing component) and the quadrature-axis stator current i_q (torque-producing component) it is necessary to cancel the effect of these coupling terms at the output of the current PI regulator [24]. However, the equations of the stator voltage components as shown in (3.11) are coupled. The direct axis component V_d also depends on i_q, and the quadrature axis component V_q also depends on i_d. The stator voltage components V_d and V_q cannot be considered as decoupled control variables for the rotor flux and electromagnetic torque. The stator currents i_d and i_q

can only be independently controlled (decoupled control) if the stator voltage equations are decoupled, so these stator current components are indirectly controlled by controlling the terminal voltages of the synchronous motor.

The equations of the stator voltage components in the d, q reference frame can be reformulated and separated into two components: linear components and decoupling components. The decoupling components are evaluated from the stator voltage equations. They eliminate cross-coupling for current control loops at a given motor operating point. Linear components $V_d^{\mathrm{L}}$and V_q^{L} are set by the outputs of the current controllers.

$$\begin{aligned} V_q &= V_q{}^{L} + V_q{}^{D} \\ V_d &= V_d{}^{L} - V_d{}^{D} \end{aligned} \tag{3.30}$$

where

$$\begin{aligned} V_q{}^{L} &= (R_s + L_q \frac{d}{dt}) i_q \\ V_d{}^{L} &= (R_s + L_d \frac{d}{dt}) i_d \end{aligned} \tag{3.31}$$

and

$$\begin{aligned} V_q{}^{D} &= \omega_r L_d i_d + \omega_r \psi_m \\ V_d{}^{D} &= \omega_r L_q i_q \end{aligned} \tag{3.32}$$

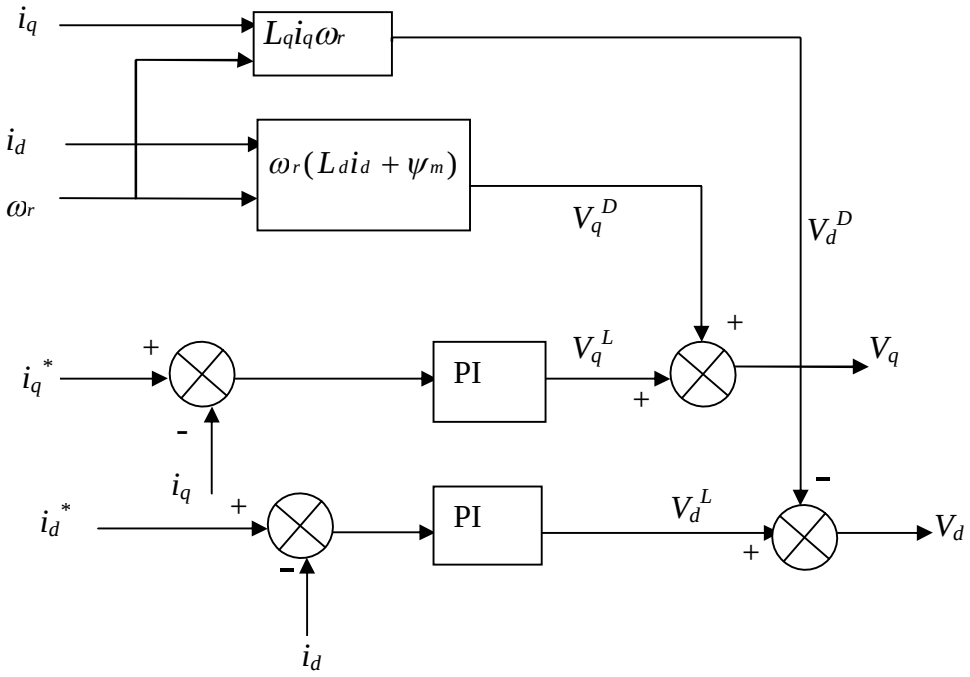

Figure 3.6: Voltage decoupling.

CHAPTER FOUR
CONTROL OF PMSM DRIVES

4.1 PMSM Drive System

Rotor position information is very crucial for field oriented (vector) control. The coordinate transformation uses the value of the rotor position in order to handle the stator current vector projection in a rotating frame. The electrical position is not directly used in this transform but the sine and cosine values of it are used.

Whether the control scheme is sensor based or sensor-less, position of the rotor is required. Control of PMSM can be categorized as sensor based and sensor-less control.

1) **Sensor based control**: in this control method, sensors are used to indicate the position of the rotor, for instance incremental encoder, absolute encoder, resolver etc. By using mechanical sensors, it is simple to measure speed and position for feedback to the controller. Moreover, controller design complexity is not that much. However, using sensor-based control increases volume, weight of the system, connection parts between motor and controller. Mechanical sensors have noise and they need space on the shaft of the motor for position measurement. It also increases the overall cost of the drive system.

2) **Sensor-less Control**: position of the rotor is estimated using algorithms. It has got some advantages. To mention; it overcomes the drawbacks of Sensor based control, it has better efficiency and lower cost without position transducer and it is reliable and faster response control method. On the contrary this control system has got some demerits. This includes sophisticated design (e.g. Kalman filter), some methods fail at standstill (e.g. Back-emf method) and expensive for low cost applications and it will take time to develop.

This thesis is totally dedicated on sensor based control of permanent magnet synchronous motor because of advantage mentioned above and the simplicity when compare to sensor less control.

A conceptual drive system is pictured in Figure 4.1 There, a speed, and current command is input to the drive system. The Controller implements feedback control based on mechanical sensors**.** The Speed controller outputs command for the Current Controller. The current controller block converts its input commands into commands for the power converter using SVPWM. The power converter block imposes the desired electrical signals onto the PMSM machine with the connected load.

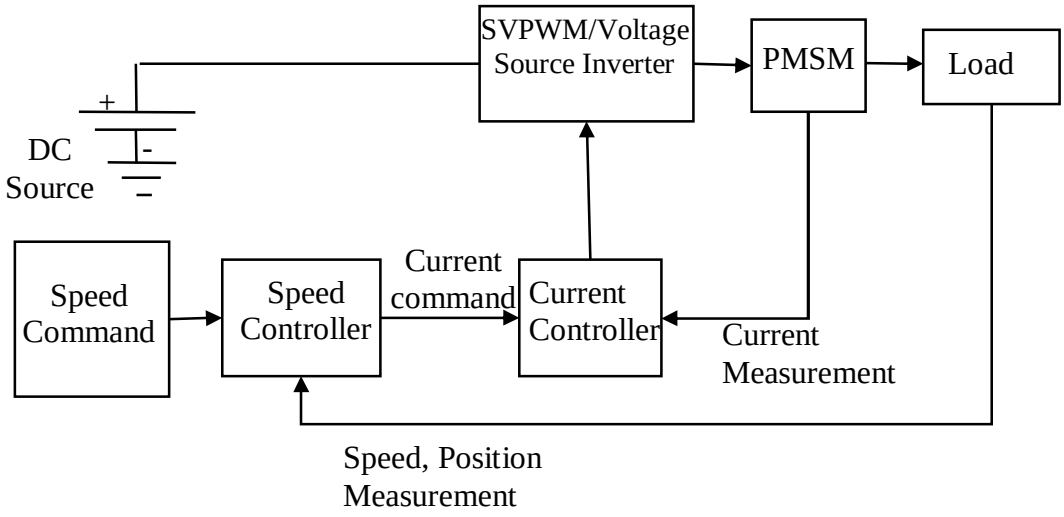

Figure 4.1: Block Diagram of PMSM drive system.

4.2 Inverters and Their Control

The subsystem that made the widespread possible use of permanent magnet (PM) drives is the standard power electronic converter module. To provide variable speed in the machine, variable frequency of the stator currents is required, which is achieved with an inverter. The inverter requires a dc voltage input, which, in a majority of the cases, is obtained from an AC supply by rectification with a diode bridge.

4.2.1 Power Devices

Improvements in fast switching power devices have led to an increased interest in voltage source inverters (VSI) with pulse width modulation control (PWM). Some of the popular power devices available today are diodes, metal oxide semiconductor field-effect transistors

(MOSFETs), and insulated gate bipolar transistors (IGBTs). These devices are commonly used in PMSM drives.

4.2.2 DC Input Source

PMSM drives require variable voltage/current input at variable frequency to deliver variable speed operation. As the utility power source has constant frequency and voltage, it cannot be directly used in these machines. As a result there must be a power conversion process to obtain a variable voltage/current, variable frequency power supply from a fixed frequency, and voltage ac power source.

The power conversion process involves first a utility AC to variable or fixed DC conversion (rectification) and then a DC to variable voltage/current, variable frequency AC conversion (inversion). The rectifier may be controlled or uncontrolled type. The uncontrolled rectifier with diodes only provides a constant DC voltage. The controlled rectifier with self-commutating devices provides a variable DC voltage. In spite of its higher cost and complexity in control, this is upcoming in a few applications where its operational flexibility in providing variable voltage, AC input current shaping, and output ripple reduction are highly required. The inverter stage consists of self-commutating devices such as MOSFETs or IGBTs and only six devices are required.

4.2.3 Voltage Source Three-Phase Inverter

Voltage Source Inverters are devices that convert a DC voltage to AC voltage of variable frequency and magnitude. Usually the motor is fed from a voltage source inverter with current control. The control is performed by regulating the flow of current through the stator of the motor. Current controllers are used to generate gate signals for the inverter. Proper selection of the inverter devices and selection of the control technique will guarantee the efficiency of the drive.

The output voltage could be fixed or variable at a fixed or variable frequency. A variable output voltage can be obtained by varying the input DC voltage and maintaining the gain of the inverter constant. On the other hand, if the DC input voltage is fixed and is not controllable, a variable output voltage can be obtained by varying the gain of the inverter,

which is normally accomplished by pulse width modulation (PWM) control within the inverter.

Three phase inverters consist of six power switches connected to a DC voltage source as shown in figure 4.2. V_a, V_b and V_c are the output voltages applied to the stator windings of a motor. Q1 through Q6 are the six power transistors that shape the output, which are controlled by a, a', b, b', c and c'. For AC motor control, when an upper transistor is switched on, i.e., when a, b or c is 1, the corresponding lower transistor is switched off, i.e., the corresponding a', b' or c' is 0. That means, tuning the upper line switch on requires turning off the lower line switch and vice versa. The on and off states of the upper transistors Q_1, Q_3 and Q_5, or equivalently, the states of a, b and c, is sufficient to evaluate the output voltage.

To understand its basic operation, assume the DC link voltage is constant in the three phase inverter circuit. Each of the phase leg is independently operated. The line voltages can be derived from the phase voltages as:

$$V_{ab} = V_{an} - V_{bn} \tag{4.1}$$

$$V_{bc} = V_{bn} - V_{cn} \tag{4.2}$$

$$V_{ca} = V_{cn} - V_{an} \tag{4.3}$$

where

V_{ab}, V_{bc}, and V_{ca} are the various line voltages

V_{an}, V_{bn}, and V_{cn} are the phase voltages

From these equations, the phase voltages are derived assuming that the system is balanced, i.e., the sum of the phase currents and voltages is equal to zero. The phase voltages in terms of the line voltages are given as:

$$V_{an} = \frac{V_{ab} - V_{ca}}{3} \tag{4.4}$$

$$V_{bn} = \frac{V_{bc} - V_{ab}}{3} \tag{4.5}$$

$$V_{cn} = \frac{V_{ca} - V_{bc}}{3} \tag{4.6}$$

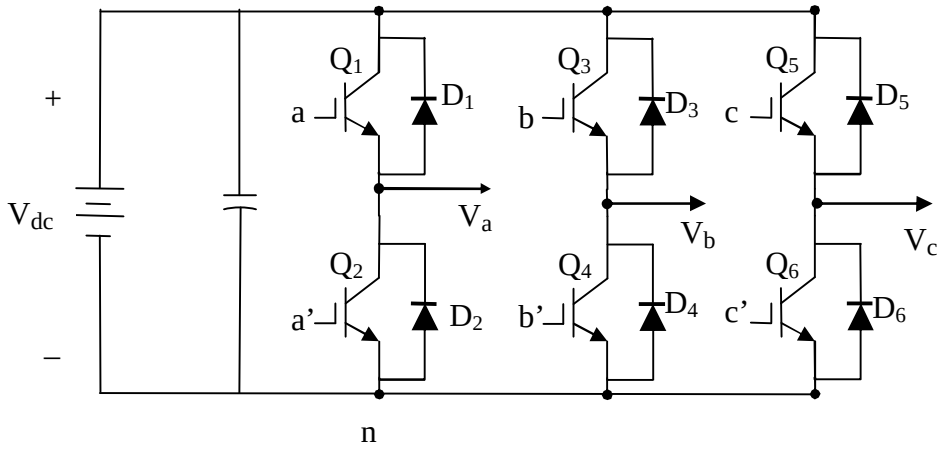

Figure 4.2: Three Phase Inverter.

From the inverter shown in Figure 4.2, the terminal voltage of phase a, V_a, with respect to negative of the dc supply is considered and it is determined by a set of switches, Sa, consisting of a and a' as shown in Table 4.1

Table 4 1: Switching States of inverter phase leg a

Switching States of inverter phase leg a			
a	a'	Sa	V_a
On	Off	1	V_{dc}
Off	On	0	0

When the switching devices a and a' and their antiparallel diodes are off, V_a is indeterminate. Such a situation is not encountered in practice and hence has not been considered. The switching of S_b and S_c sets for line b and c can be similarly derived.

The total number of switching states possible with S_a, S_b, and S_c are eight and they are elaborated in the Table 4.2 using the relationships (Equations (4.4) through (4.6)) containing the phase and line-to-line voltages. The α- and β-axes voltages (stationary axis) can be derived from the phase voltages as:

$$V_\alpha = V_{an}$$
$$V_\beta = \frac{1}{\sqrt{3}}(V_{cn} - V_{bn}) = \frac{1}{\sqrt{3}}V_{cb} \tag{4.7}$$

4.3 Position Sensor

Accurate measurement of rotor position is needed for applying a vector control to AC motors. This requires the development of devices for position measurement. There are different types of rotor position measuring device like resolver, tachogenerator, and optical encoder. The ones most commonly used for motors are encoders and resolver.

4.3.1 Optical Encoder

Encoders transform rotary movement into a sequence of electrical pulses. An encoder consists of a rotating disk, a light source, and a photo detector (light sensor). The disk, is mounted on the rotating shaft, has coded patterns of opaque and transparent sectors. As the disk rotates, these patterns interrupt the light emitted onto the photo detector, generating a digital pulse or output signal. It is the most popular type of encoder. Optical encoders offer the advantages of digital interface [32]. There are two types of optical encoders, *incremental* encoder and *absolute* encoder. In this thesis a simulated incremental quadrature pulse encoder is used.

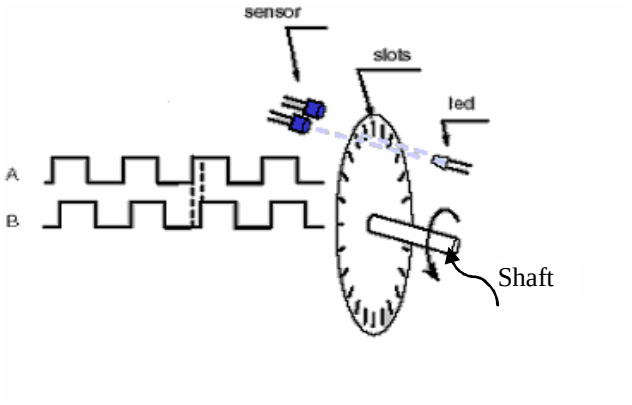

Figure 4.3: Optical encoder [26].

Incremental Quadrature Encoders

The disk of an incremental encoder is patterned with a single track of lines around its periphery. The disk count is defined as the number of dark/light line pairs that occur per revolution ("cycles / revolution"). The number of square wave cycles produced per one turn of the shaft is called the encoder resolution.

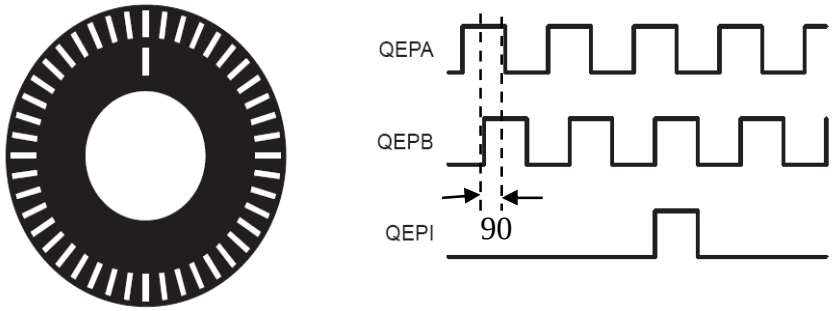

Figure 4.4: Output pulses of incremental encoder [25]

As a rule, a second track is added to generate a signal that occurs once per revolution (QEPI), which can be used to indicate an absolute position. The precision of the encoder is fixed by its code disk but it can be increased by detecting the up and down transitions on both the A and B channels. To derive direction information, the lines on the disk are read out by two different photo-elements that "look" at the disk pattern with a mechanical shift of ¼ of a cycle (90 degrees) between them. As the disk rotates, the two photo-elements generate signals that are shifted 90° out of phase from each other. These are commonly called the quadrature "A" and "B" signals. The clockwise direction for most encoders is defined as the "A" channel going positive before the "B" channel [33].

4.4 Pulse Width Modulation (PWM)

PWM control is the first scheme to be applied on a large scale for control of inverter. During that time, the understanding of the AC motor drive and its performance was evolving. There was fair understanding of steady-state operation and its control but limited knowledge of transient operation, resulting in instability and inverter failure because of immense dynamic currents being drawn during the load or speed transients [1].

4.4.1 Sinusoidal Pulse width Modulation

Sinusoidal PWM has been very popular technique used in AC motor control. This relatively unsophisticated method employs a triangular carrier wave compared with a sine wave and the points of intersection determine the switching points of the power devices in the inverter. However, this method is unable to make full use of the inverter’s supply voltage and the

asymmetrical nature of the PWM switching characteristics produces relatively high harmonic distortion in the supply.

Figure 4.5 shows circuit model of a single-phase inverter with a center-taped grounded DC bus and figure 4.6 illustrates principle of pulse width modulation.

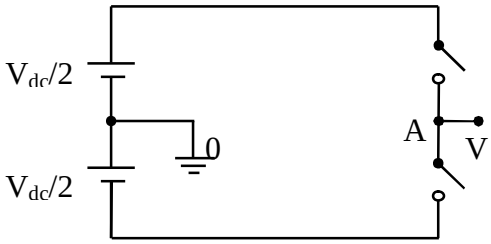

Figure 4.5: Single-phase inverter.

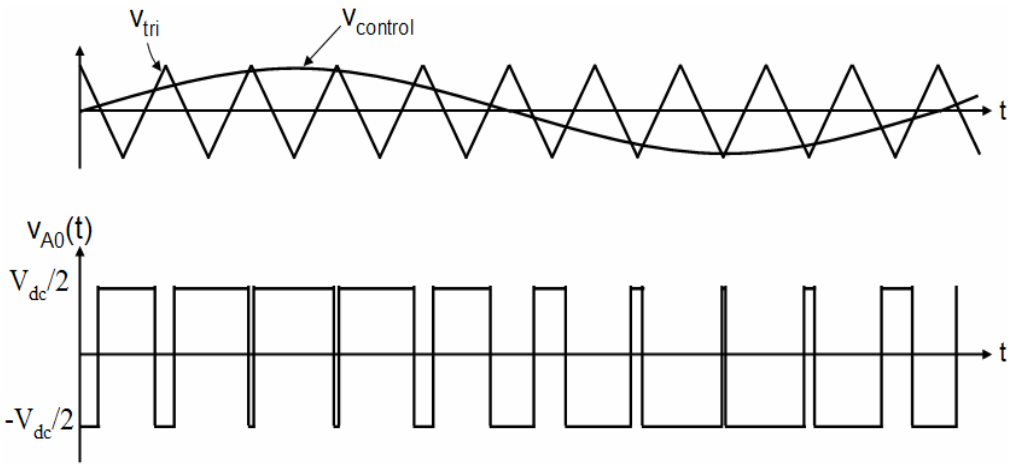

Figure 4.6: Sinusoidal Pulse width modulation.

As showed in Figure 4.6, the inverter output voltage is determined in the following:

- When $V_{control} > V_{tri}$, $V_{A0} = V_{dc}/2$
- When $V_{control} < V_{tri}$, $V_{A0} = -V_{dc}/2$

4.4.2 Space Vector PWM

In the late 1960s and early 1970s, efforts were made to understand the dynamics of the ac machines. It all started on the basis that independent control of flux and torque is the characteristic of the separately excited DC motor drive that gives a very high dynamic and

steady-state performance. An equivalent control of that in AC motor drives, if found, can overcome entirely the problems associated with the dynamic transients of the motor drive [1].

The key step to this method is the understanding of the ac machines as an equivalent separately excited dc machine. This required the ac machine model to be reduced into a set of single stator and rotor windings using space phasor model. If the machine takes a single stator current space phasor, then the inverter supplying the current must be generating it as a space phasor but not simply as a set of three-phase currents. Hence the inverter may be viewed as a voltage and or current space phasor generator but not as a three-phase voltage or current generator. This understanding of the inverter as a voltage/current phasor generator further imports the notion that the inverter is not only controlling the magnitude and angular velocity but also the angular position of the voltage and current phasor as the mere fact that a space phasor is in fact consists of three these variables. The position variable that the inverter is exercising control over has the most dramatic impact on the dynamics of the motor drive [1].

Note that any voltage space phasor can by synthesized with the control of inverter switching by considering the requested voltage phasor's magnitude and position. This approach does not use individual pulse width modulators for each machine phase [1].

The relationship between the switching variable vector $[a, b, c]^t$ and the line-to-line voltage vector $[V_{ab}\, V_{bc}\, V_{ca}]^t$ of the three phase inverter in Figure 4.2 is given by equation (4.8) .

$$\begin{bmatrix} V_{ab} \\ V_{bc} \\ V_{ca} \end{bmatrix} = V_{dc} \begin{bmatrix} 1 & -1 & 0 \\ 0 & 1 & -1 \\ -1 & 0 & 1 \end{bmatrix} \begin{bmatrix} a \\ b \\ c \end{bmatrix} \tag{4.8}$$

where

[a b c] is a vector representing the upper switches of the inverter.

Also, the relationship between the switching variable vector $[a, b, c]^t$ and the phase voltage vector $[V_a V_b V_c]^t$ can be expressed below.

$$\begin{bmatrix} V_{an} \\ V_{bn} \\ V_{cn} \end{bmatrix} = \frac{V_{dc}}{3} \begin{bmatrix} 2 & -1 & -1 \\ -1 & 2 & -1 \\ -1 & -1 & 2 \end{bmatrix} \begin{bmatrix} a \\ b \\ c \end{bmatrix} \tag{4.9}$$

The on and off states of the upper power devices are opposite to the lower one. So once the states of the upper power transistors are determined, the states of lower one can be easily determined. According to equations (4.1) and (4.3) the eight switching vectors of the three upper power switches, output line to neutral voltage (phase voltage), and output line-to-line voltages in terms of DC-link V_{dc}, are given in Table 4.2.

Table 4.2: Switching vectors, phase voltages and output line to line voltages.

Voltage vectors	Switching vectors			Line to neutaral voltage			Line to line voltage			V_α	V_β
	a	b	c	V_{an}	V_{bn}	V_{cn}	V_{ab}	V_{bc}	V_{ca}		
V_0	0	0	0	0	0	0	0	0	0	0	0
V_1	1	0	0	2/3	-1/3	-1/3	1	0	-1	2/3	0
V_2	1	1	0	1/3	-1/3	-1/3	1	0	-1	1/3	$1/\sqrt{3}$
V_3	0	1	0	-1/3	2/3	-1/3	-1	1	0	-1/3	$1/\sqrt{3}$
V_4	0	1	1	-2/3	1/3	1/3	-1	0	1	-2/3	0
V_5	0	0	1	-1/3	-1/3	2/3	0	-1	1	-1/3	$-1/\sqrt{3}$
V_6	1	0	1	1/3	-2/3	1/3	1	-1	0	1/3	$-1/\sqrt{3}$
V_7	1	1	1	0	0	0	0	0	0	0	0

(Note that the respective voltage should be multiplied by V_{dc})

Principle of Space Vector PWM

- ✓ Treats the sinusoidal voltage (reference voltage) as a constant amplitude vector rotating at constant frequency.
- ✓ This PWM technique approximates the reference voltage V_{ref} by a combination of the eight switching patterns (V_0 to V_7).

- ✓ Coordinate Transformation (abc reference frame to the stationary α-β frame). That is a three-phase voltage vector is transformed into a vector in the stationary α-β coordinate frame represents the spatial vector sum of the three phase voltage.
- ✓ The vectors (V_1 to V_6) divide the plane into six sectors (each sector: 60 degrees).
- ✓ V_{ref} is generated by two adjacent non-zero vectors and two zero vectors.

Implementation of Space Vector PWM

To implement the space vector PWM, the voltage equations in the *abc* reference frame must be transformed into the stationary αβ reference frame that consists of the horizontal (α) and vertical (β) axes, as a result, six non-zero vectors and two zero vectors are possible. Six nonzero vectors ($V_1 – V_6$) shape the axes of a hexagonal as depicted in Figure 4.7, and feed electric power to the load or DC link voltage is supplied to the load. The objective of space vector PWM technique is to approximate the reference voltage vector V_{ref} using the eight switching patterns. One simple method of approximation is to generate the average output of the inverter in a small period, T_z to be the same as that of V_{ref} in the same period.

Consider that voltage phasor V_{ref} is commanded. Its position is in between two switching voltage vectors, say V_1 and V_2, and has a relative phase of α from V_1, as shown in Figure 4.7. The commanded voltage phasor can only be realized with the use of the neighboring switching voltage vectors and in this case V_1 and V_2. Taking these switching vectors for a fraction of time as it is not possible to take the fraction of them, and then combining them through the load gives the desired command space voltage phasor.

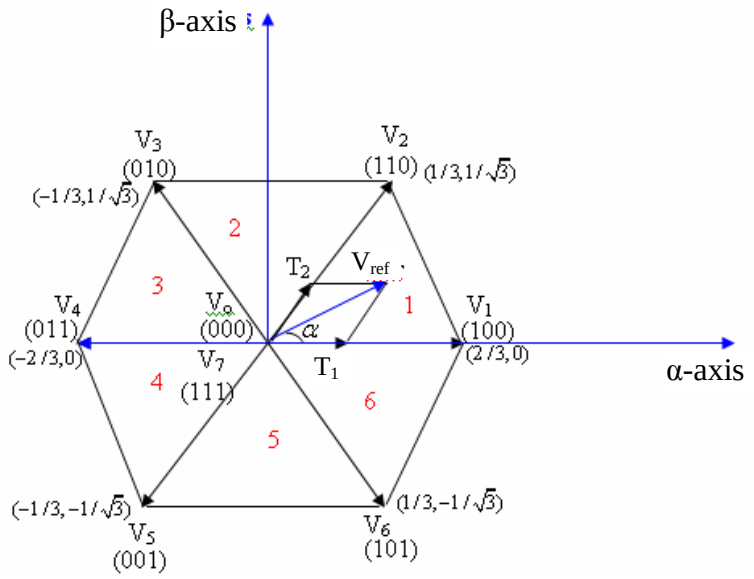

Figure 4.7: Basic switching vectors, sectors and a reference vector.

Therefore, space vector PWM can be implemented by the following steps:

- ✓ **Step 1**. Determine V_α, V_β, V_{ref}, and angle (α) to determine the specific sector.
- ✓ **Step 2**. Determine time duration T_1, T_2, T_0 for the specific sector where T_1, T_2 are the respective time for which the basic space vectors V_1 and V_2 should be applied within the time period T_z and T_0 is the course of time for which the null vectors V_0 and V_7 are applied.
- ✓ **Step 3**. Determine the switching time of each transistor (S_1 to S_6)

Step 1: Determine V_α, V_β, V_{ref}, and angle (α)

Using the co-ordinate transformation to 2-Φ stationary reference frame in Figure 4.8, the V_α, V_β, V_{ref}, and angle (α) can be determined as follows:

$$\begin{aligned} V_\alpha &= V_{an} - V_{bn}\cdot\cos(60) - V_{cn}\cdot\cos(60) \\ &= V_{an} - \frac{1}{2}V_{bn} - \frac{1}{2}V_{cn} \end{aligned} \tag{4.10}$$

$$\begin{aligned} V_\beta &= 0 + V_{bn}\cdot\cos(30) - V_{cn}\cdot\cos(30) \\ &= \frac{\sqrt{3}}{2}V_{bn} - \frac{\sqrt{3}}{2}V_{cn} \end{aligned} \tag{4.11}$$

Therefore, the above equations can be summarized in matrix form as follows.

$$\begin{bmatrix} V_\alpha \\ V_\beta \end{bmatrix} = \begin{bmatrix} 1 & -\frac{1}{2} & -\frac{1}{2} \\ 0 & \frac{\sqrt{3}}{2} & -\frac{\sqrt{3}}{2} \end{bmatrix} \begin{bmatrix} V_{an} \\ V_{bn} \\ V_{cn} \end{bmatrix} \tag{4.12}$$

The reference space vector voltage crossing every sector is derived as:

$$\left|\overline{V}_{ref}\right| = \sqrt{V_\alpha{}^2 + V_\beta{}^2} \tag{4.13}$$

The current sector in which the reference voltage vector found is determined by equation (4.14).

$$\alpha = \tan^{-1}\left(\frac{V_\beta}{V_\alpha}\right) = \omega t = 2\pi f t \tag{4.14}$$

where

f is the fundamental frequency at which the reference voltage rotates.

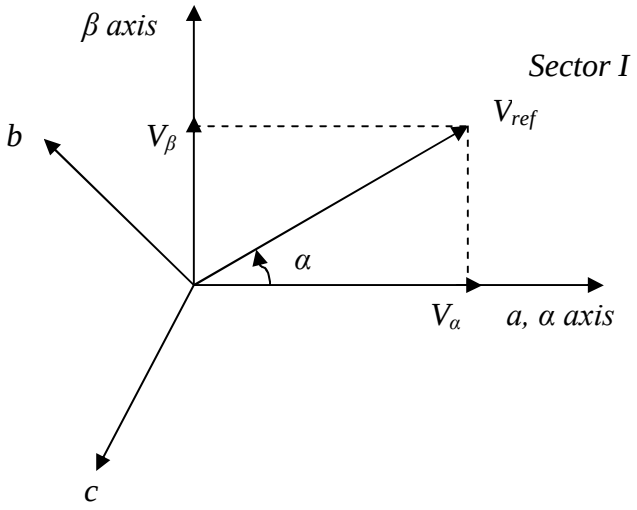

Figure 4.8: Voltage space vector and its components in (abc axis) [23].

Step 2: Determine time duration T_1, T_2, T_0

From Figure 4.8, the switching time duration can be calculated as follows:

Switching time duration at Sector 1:

$$\int_0^{Tz} \overline{V}_{ref}\, dt = \int_0^{T_1} \overline{V}_1 dt + \int_{T_1}^{T_1+T_2} \overline{V}_2 dt + \int_{T_1+T_2}^{Tz} \overline{V}_0 dt \tag{4.15}$$

$$\therefore Tz \cdot \overline{V}_{ref} = \left(T_1 \cdot \overline{V}_1 + T_2 \cdot \overline{V}_2\right) \tag{4.16}$$

The average voltage for the first sector which is made by vectors V_0, V_1, V_2, and V_7 is given by equation (4.17). (Where, $0 \le \alpha \le 60$)

$$\Rightarrow T_z \cdot \left|\overline{V}_{ref}\right| \cdot \begin{bmatrix}\cos(\alpha)\\ \sin(\alpha)\end{bmatrix} = T_1 \cdot \frac{2}{3} \cdot V_{dc} \cdot \begin{bmatrix}1\\ 0\end{bmatrix} + T_2 \cdot \frac{2}{3} \cdot V_{dc} \cdot \begin{bmatrix}\cos(\pi/3)\\ \sin(\pi/3)\end{bmatrix} \tag{4.17}$$

$$\therefore T_1 = T_z \cdot a \cdot \frac{\sin(\frac{\pi}{3} - \alpha)}{\sin(\pi/3)} \tag{4.18}$$

$$\therefore T_2 = T_z \cdot a \cdot \frac{\sin(\alpha)}{\sin(\pi/3)} \tag{4.19}$$

$$T_0 = T_z - (T_1 + T_2), \tag{4.20}$$

where

$$T_z = \frac{1}{f_z} \quad and \quad a = \frac{\left|\overline{V}_{ref}\right|}{\frac{2}{3}V_{dc}} \tag{4.21}$$

T_1, T_2 are the switching time durations of vectors V_1 and V_2 respectively.

T_0 is the time duration of the zero vector.

T_z is the time period for which one sector is applied.

Switching time duration at any sector is given by the following equations:

$$\begin{aligned} T_n &= \frac{\sqrt{3} \cdot T_z \cdot \left|\overline{V}_{ref}\right|}{V_{dc}} \left(\sin\left(\frac{\pi}{3} - \alpha + \frac{n-1}{3}\pi \right) \right) \\ &= \frac{\sqrt{3} \cdot T_z \cdot \left|\overline{V}_{ref}\right|}{V_{dc}} \cdot \sin\left(\frac{n}{3}\pi - \alpha \right) \\ &= \frac{\sqrt{3} \cdot T_z \cdot \left|\overline{V}_{ref}\right|}{V_{dc}} \left(\sin\frac{n}{3}\pi \cdot \cos\alpha - \cos\frac{n}{3}\pi \cdot \sin\alpha \right) \end{aligned} \tag{4.22}$$

$$T_{n+1} = \frac{\sqrt{3} \cdot T_z \cdot \left|\overline{V}_{ref}\right|}{V_{dc}} \left(\sin\left(\alpha - \frac{n-1}{3}\pi \right) \right)$$
$$= \frac{\sqrt{3} \cdot T_z \cdot \left|\overline{V}_{ref}\right|}{V_{dc}} \left(-\cos\alpha \cdot \sin\frac{n-1}{3}\pi + \sin\alpha \cdot \cos\frac{n-1}{3}\pi \right) \quad (4.23)$$

$$T_0 = T_z - (T_n + T_{n+1}), \quad (4.24)$$

where

n = 1 through 6(sector I to VI) and $0 \leq \alpha \leq 60$

The method used to approximate the desired stator reference voltage with only eight possible states of switches is to combine adjacent vectors of the reference voltage and to determine the time of application of each adjacent vector as shown in Figure 4.9 for the first sector.

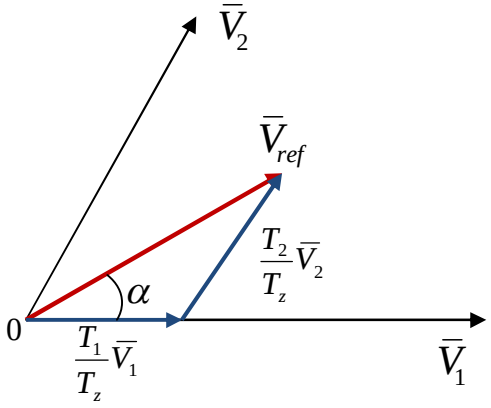

Figure 4.9: Reference voltage as a combination of adjacent vectors in sector I [23].

Step 3: Determine the switching time of each transistor (S_1 to S_6)

Figure 4.10 shows space vector PWM switching patterns for sector I and II.

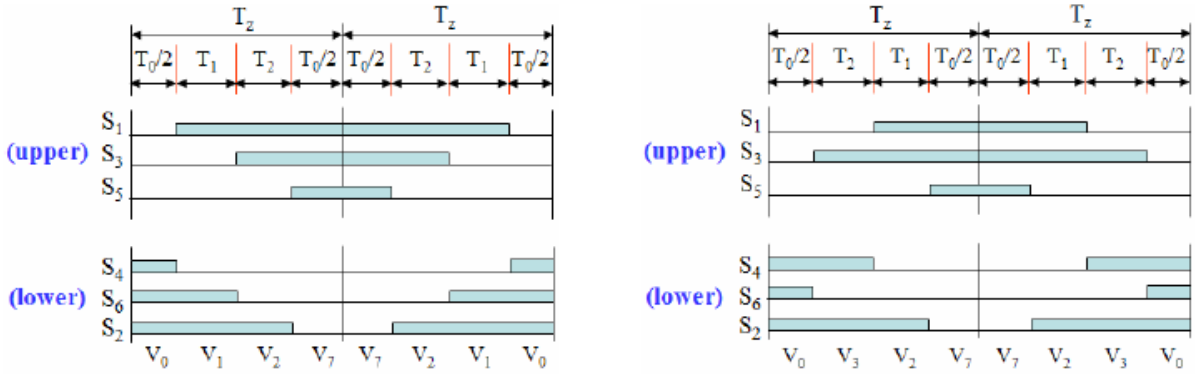

(a) Sector I (b) Sector II

Figure 4.10: Space Vector PWM switching patterns for the first two sectors.

Based on Figure 4.10, the switching time at each sector is summarized in Table 4.3.

Table 4.3: Switching Time Calculation at Each Sector.

Sector	Upper Switches(S_1,S_3,S_5)	Lower Switches(S_4,S_6,S_2)
1	$S_1=T_1 + T_2 + T_0/2$ $S_3 = T_2 + T_0/2$ $S_5 = T_0/2$	$S_4 = T_0/2$ $S_6 = T_1 + T_0/2$ $S_2 = T_1 + T_2 + T_0/2$
2	$S_1 = T_1 + T_0/2$ $S_3 = T_1 + T_2 + T_0/2$ $S_5 = T_0/2$	$S_4 = T_2 + T_0/2$ $S_6 = T_0/2$ $S_2 = T_1 + T_2 + T_0/2$
3	$S_1 = T_0/2$ $S_3 = T_1 + T_2 + T_0/2$	$S_4 = T_1 + T_2 + T_0/2$ $S_6 = T_0/2$

	$S_5 = T_2 + T_0/2$	$S_2 = T_1 + T_0/2$
4	$S_1 = T_0/2$ $S_3 = T_1 + T_0/2$ $S_5 = T_1 + T_2 + T_0/2$	$S_4 = T_1 + T_2 + T_0/2$ $S_6 = T_2 + T_0/2$ $S_2 = T_0/2$
5	$S_1 = T_2 + T_0/2$ $S_3 = T_0/2$ $S_5 = T_1 + T_2 + T_0/2$	$S_4 = T_1 + T_0/2$ $S_6 = T_1 + T_2 + T_0/2$ $S_2 = T_0/2$
6	$S_1 = T_1 + T_2 + T_0/2$ $S_3 = T_0/2$ $S_5 = T_1 + T_0/2$	$S_4 = T_0/2$ $S_6 = T_1 + T_2 + T_0/2$ $S_2 = T_2 + T_0/2$

Comparison SVPWM and Sinusoidal PWM

- Space Vector PWM generates less harmonic distortion in the output voltage or currents in comparison with sine PWM.
- Space Vector PWM provides more efficient use of supply voltage in comparison with sine PWM. Voltage Utilization: Space Vector PWM $= 2/\sqrt{3}$ times of Sine PWM.
- In sine PWM the locus of the reference vector is the inside of the circle with the radius of $1/2\ V_{dc}$.
- In Space Vector PWM the locus of the reference vector is the inside of a circle with radius of $1/\sqrt{3}\ V_{dc}$.

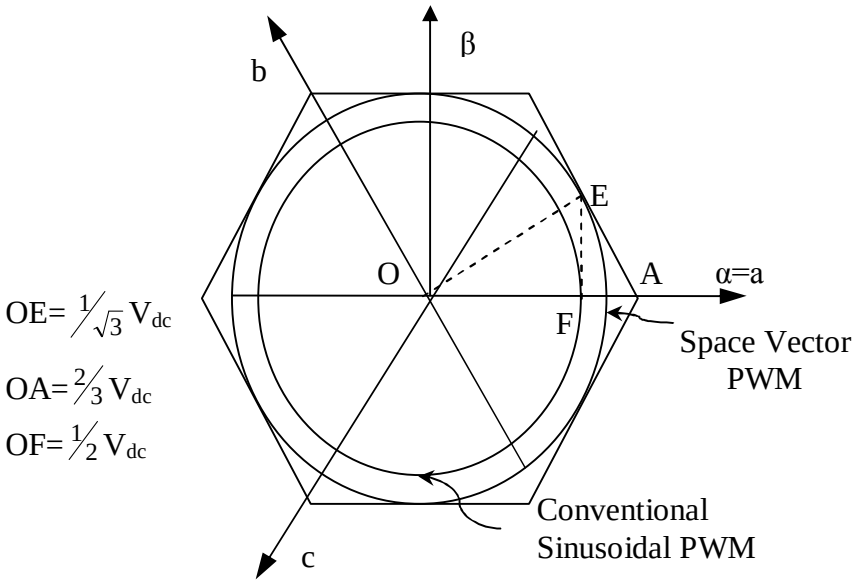

Figure 4.11: Comparison SVPWM and Sinusoidal PWM.

4.5 Controller Design

4.5.1 Introduction to Fuzzy-Logic

The fuzzy logic is a class of artificial intelligence with a recent history and application. The concept of fuzzy logic was first introduced by 1965 by a computer scientist Lotfy Zadeh, a professor at the University of California at Berkley, and presented not as a control methodology, but as a way of processing data by allowing partial set membership rather than crisp set membership or non-membership. He argued that human thinking is often fuzzy, vague, or imprecise in nature, and, therefore cannot be represented by yes (1) or no (0). Fuzzy logic allows the programmer to deal with natural, “linguistic sets” of states, such as very fast, fast, slow, etc. Fuzzy-logic provides a simple way to arrive at a definite conclusion based upon vague, ambiguous, imprecise, noisy, or missing input information. Its approach to control problems mimics how a person would make decisions, much faster [4][34].

Fuzzy logic incorporates a simple, rule-based IF X AND Y THEN Z approach to a solving control problem rather than attempting to model a system mathematically. The FL model is experimentally-based, relying on an operator's experience rather than their technical understanding of the system. Figure 4.12 and 4.13 compares the membership functions (μ(x)) of element x in the universe of discourse for classical sets and fuzzy sets.

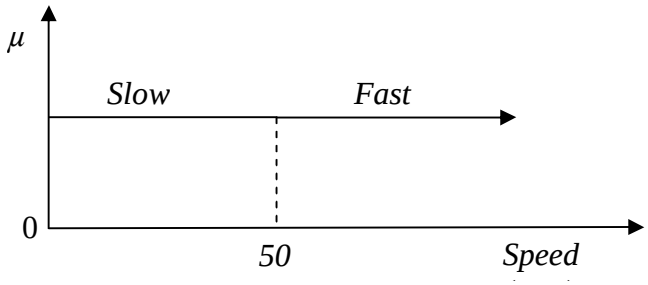

Figure 4.12: Classical logic.

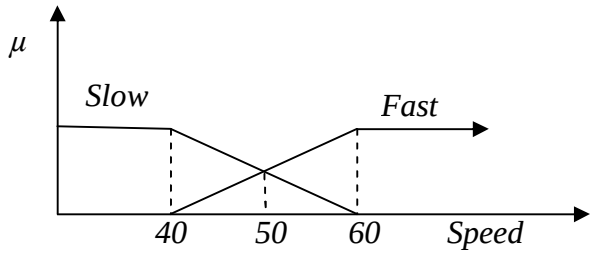

Figure 4.13: Fuzzy logic.

1. Fuzzy Sets

Define a universe of discourse, X, as a collection of objects all having the same characteristics. The individual elements in the universe X will be denoted as *x*. In classical, or crisp, sets the transition for an element in the universe between membership and nonmembership in a given set is abrupt and well-defined (said to be ‘‘crisp’’). For an element in a universe that contains fuzzy sets, this transition can be gradual. This transition among various degrees of membership can be lead to the fact that the boundaries of the fuzzy sets are vague and ambiguous [34]. Hence, membership of an element from the universe in this set is measured by a function that attempts to describe vagueness and ambiguity. Elements of a fuzzy set are mapped to a universe of membership values (degree to which a quality is possessed) using a function-theoretic form in the range of [0, 1]. If an element in the universe, say x, is a member of fuzzy set A, then this mapping is given by $\mu(x) \in [0, 1]$.

2. Fuzzy Set Operations

Define three fuzzy sets A, B, and C on the universe X. For a given element *x* of the universe, the following function-theoretic operations for the set-theoretic operations of union, intersection, and complement are defined for A, B, and C on X.

Union

$$\mu_{A\cup B}(x) = \mu_A(x) \vee \mu_B(x) = \max(\mu_A(x), \mu_B(x)) \tag{4.25}$$

Intersection

$$\mu_{A\cap B}(x) = \mu_A(x) \wedge \mu_B(x) = \min(\mu_A(x), \mu_B(x)) \tag{4.26}$$

Complement

$$\mu_{\bar{A}}(x) = 1 - \mu_A(x) \tag{4.27}$$

Excluded middle axioms, extended for fuzzy sets, are expressed by $A \cup A \neq X$ (axiom of excluded middle) and $A \cap A \neq \emptyset$ (axiom of contradiction).

3. Linguistic Variables

Cognitive scientists tell us that humans base their thinking primarily on conceptual patterns and mental images rather than on any numerical quantities. Furthermore, humans communicate with their own natural language by referring to previous mental images with rather vague but simple terms. A linguistic variable associates words or sentences with a measure of belief functions, also called membership function. The set of values that it can take is called term set. Each value in the set is a fuzzy variable defined over a base variable. The base variable defines the Universe of discourse for all the fuzzy variables in the term set [4].

4. Membership Function (MF)

Membership function is a function that changes the crisp variables (classical sets) in to fuzzy sets. All information contained in a fuzzy set is described by its membership function. MFs describe the degree of confidence of all elements in the universe of discourse to each fuzzy set. The shape of Membership functions depends on the system that is to be controlled. Trapezoidal (or Triangular) shapes are the most frequently used membership functions. Other shapes may be able to reflect natural phenomena, but may require complex equations to model, which can affect drastically increase the size and complexity of the fuzzy system. Every element in the universe of discourse is a member of the fuzzy set to some grade, May be even zero. The function that ties a number to each element x of the universe is called the membership function μ(x).

4.5.2 Fuzzy Logic Controller (FLC)

The basic idea behind fuzzy logic control is to incorporate the experience of a human operator in the design of a controller in controlling a process whose input-output relationship is described by a collection of fuzzy control rules (e.g. IF-THEN rules) involving linguistic variables. The design procedure of Fuzzy Logic Controller (FLC) is based upon knowledge derived from imprecise heuristic knowledge of experienced operator, does not require precise knowledge of the system model [4] [8]. A Fuzzy Logic Controller usually consists of:

- A **Fuzzification** unit which maps measured inputs of crisp value into fuzzy linguistic values to be used by a fuzzy reasoning mechanism.
- A **Knowledge base** (**KB**) which is the collection of expert control knowledge required to achieve the control objective.
- A **Fuzzy reasoning mechanism (inference engine)** that performs various fuzzy logic operations to infer the control action for the given fuzzy inputs.
- A **Defuzzification** unit which converts the inferred fuzzy control action into the required crisp control values to be entered into the system process.

a. Fuzzification

Fuzzification is the process of making a crisp quantity fuzzy. It transforms the physical values of the error signal, rate of change of error which is input to the fuzzy logic controller, into a fuzzy set consisting of an interval for the range of the input values and an associate membership function describing the degrees of the confidence of the input belonging to this range. The conversion process is performed by a membership function. The purpose of this fuzzification step is to make the input physical signal compatible with the fuzzy control rule base in the core of the controller.

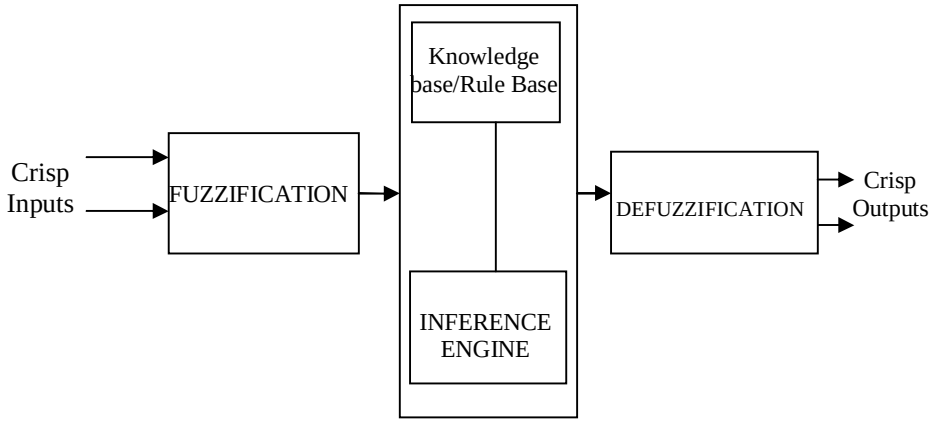

Figure 4.14: General Structure of Fuzzy Logic Controller.

b. Knowledge Base

The knowledge base of a fuzzy logic controller consists of a data base and a rule Base. The basic function of the data base is to provide the necessary information for the proper functioning of the fuzzification, the rule base and the defuzzification units. This information includes:

- ✓ The meaning of the linguistic values of the membership functions of the Input variables and the control output variables.
- ✓ Physical domains and their normalized counterparts together with the normalization, denormalization and scaling factors.
- ✓ The type of the membership functions of a fuzzy set.

The rule base is the way that expert knowledge is described for fuzzy logic controller. The majority of fuzzy logic control systems are knowledge-based systems in that their fuzzy logic controllers are described by fuzzy IF (antecedent)-THEN (consequent) rules, which have to be established based on experience of the controllers. The basic function of the rule base is to represent the expert knowledge in a form of if-then rule structure. The power of fuzzy rule-based systems is their ability to yield ‘‘good’’ results with reasonably simple mathematical operations.

C. Inference Mechanism

In order to draw conclusions from a rule base, we need a mechanism that can produce an output from a collection of IF-THEN rules. This is done using the computational rule of inference. The Inference Mechanism provides the mechanism for referring to the rule base such that the appropriate rules are fired. The two most commonly used inference procedures in FLC are Mamdani's Max-Min and Max-Algebraic Product (or Max-Dot) composition. The inference or firing with this fuzzy relation is performed via the operations between the fuzzified crisp input and the fuzzy relation representing the meaning of the overall set of rules. As a result of the composition, one obtains the fuzzy set describing the fuzzy value of the overall control output. In this thesis a Mamdani's Max-min composition inference method is used.

Max-Min composition:

Consider a simple system where each rule comprises two antecedents and one consequent. A fuzzy system with two non-interactive inputs $x1$ and $x2$ (antecedents) and a single output y (consequent) are described by a collection of n linguistic IF-THEN rules.

$$\text{IF } x1 \text{ is } A_1^{(k)} \text{ and } x_2 \text{ is } A_2^{(k)} \text{ THEN } y(k) \text{ is } B^{(k)}, \quad k = 1,2,...n. \tag{4.28}$$

where

$A_1^{(k)}$ and $A_2^{(k)}$ are fuzzy sets representing the k^{th} antecedent pairs and $B^{(k)}$ are the fuzzy sets representing the k^{th} consequent.

Based on the Mamdani's max-min composition method of inference, and for a set of disjunctive rules, the aggregated output for the n rules will be given by:

$$\mu_B^{(k)}(y) = \text{Max Min}[\mu_{A1}^{(k)}(\text{input}(i)), \mu_{A2}^{(k)}(\text{input}(j))] \tag{4.29}$$

where i, j are input fuzzy set variables and y is output fuzzy set variable.

The equation in (4.29) has a simple graphical interpretation, as seen in Figure 4.15.

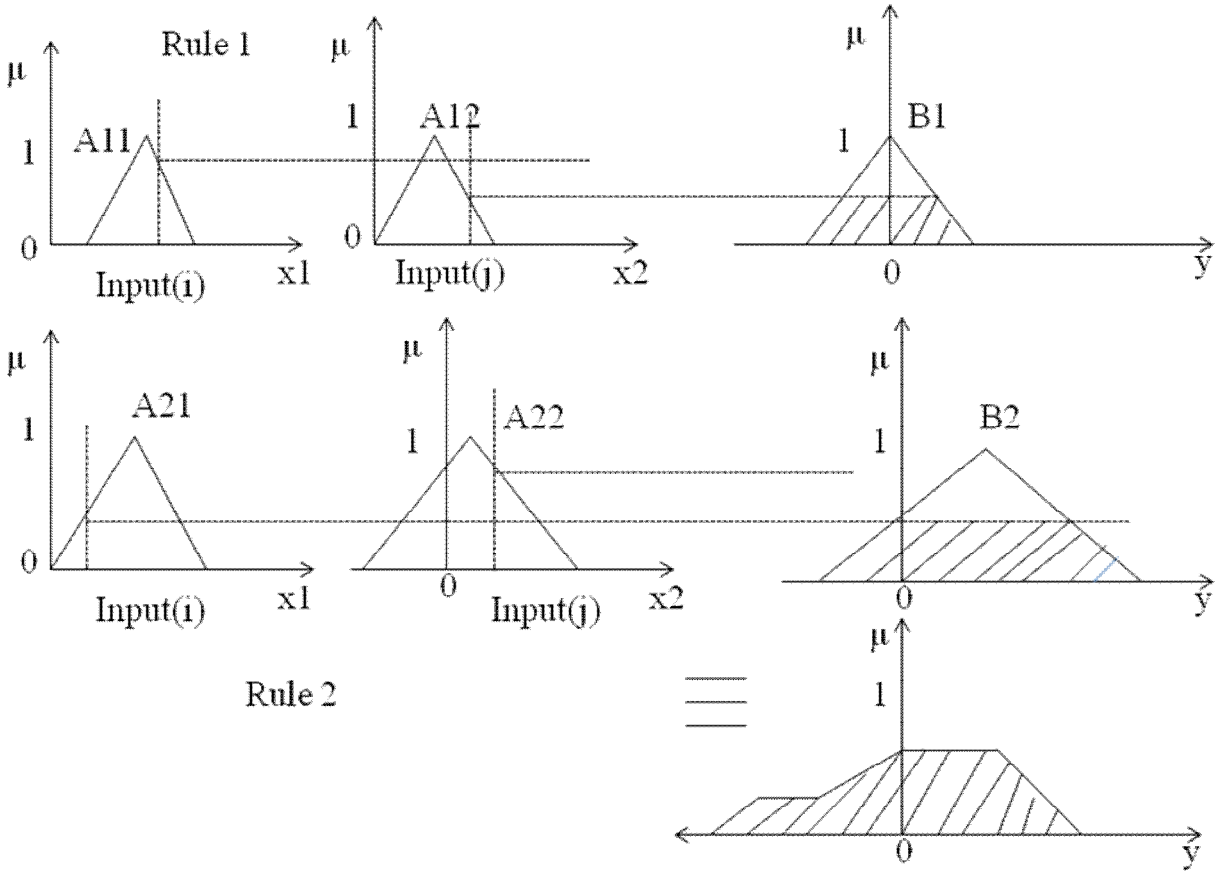

Figure 4.15: Fuzzy inferencing using Mamdani's max-min compositional operator.

The fuzzy IF-THEN rule in Figure 4.15 contains two rules. Both rules "IF x_1 is A_{11} and x_2 is A_{12} THEN y is B1" and "IF x_1 is A_{21} and x_2 is A_{22} THEN y is B_2" are intersection fuzzy set operation and take the minimum membership values of the two inputs. Then the outputs of the two rules aggregated using the union fuzzy set operation that takes the maximum membership values of each fuzzy rule outputs. For this specific example Equation (4.29) can be simplified as $\mu_B(y)$ = Max [Min (μ_{A11}(input(i)), μ_{A12}(input(j)), Min (μ_{A21}(input(i)), μ_{A22}(input(j))].

D. Difuzzification

Defuzzification unit in FLC is the inverse of the fuzzification process. It converts the fuzzy controller output fuzzy variables in to a crisp real signal. There are several commonly used, logically meaningful, and practically effective defuzzification formulas available, which are by nature weighted average formulas in various forms. Unfortunately, there is no systematic

procedure for choosing a defuzzification strategy. In this thesis a center of gravity difuzzification method is adopted for, which can reflect the overall inference information.

Center of gravity method

This procedure is the most prevalent and physically appealing of all the defuzzification methods. It is given by the algebraic expression in equation (4.30).

$$x^* = \frac{\sum \mu_x(x).x}{\sum \mu_x(x)} \tag{4.30}$$

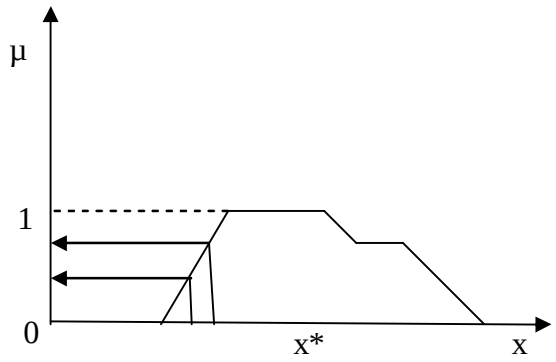

Figure 4.16: Center of gravity defuzzification method.

Design Process of FLC

- Identify controller Inputs and Outputs as the Fuzzy variables.
- Break up Inputs and Outputs into several Fuzzy Sets and label them according to the problem to be solved.
- Assign or determine a membership function (MF) for each fuzzy set.
- Choose appropriate scaling factors for the input and output variable to normalize to [0,1] or [-1,1] interval range.
- Fuzzify the inputs
- Develop the fuzzy IF-THEN rules to solve the problem.
- Choose Inference Mechanism engine procedure.
- Aggregate the fuzzy outputs of each rule.
- Choose a DEFUZZIFICATION method.
- Tune the adjustable parameters.

4.5.3 PI Controller

In process control today, more than 95% of the control loops are of PID type, most loops are actually PI control. In the control of dynamic systems, no controller has enjoyed both the success and the failure of the PID control. There is actually a great variety of types and design methods for the PID controller. The most used type of PID controller is PI controller. What is a PI controller? The acronym PI stands for **P**roportional-**I**ntegral control. Each of these, **P**, and **I** are terms in a control algorithm, and each has a special purpose. In the field of electrical drives PI regulators are employed for motor control. The variables to be controlled are position, speed, torque, and current or voltage. The fact that the measurement of these signals can contain considerable noise (high frequency) makes the PI structure without the derivative part more suitable. And in fact PI controller is enough for first order systems [35].

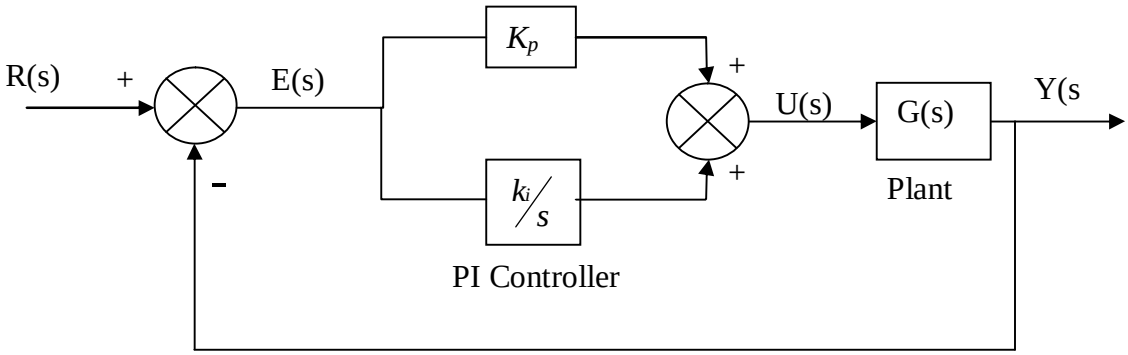

Figure 4.17: PI control System

The control signal u (t) of the PI control system in Figure 4.17 is the sum of two terms. Each of these terms is a function of the tracking error e (t). The term K_p (Proportional gain) indicates that this term is proportional to the error, and the term K_i/s is an integral term. With $K_i = 0$, the controller becomes simply a P controller which has an output that depends only on error as it is shown in equation (4.31).

$$u(t) = K_p e(t) \tag{4.31}$$

Thus at any instant time, the control is proportional to the error. It is a function of the present value of the error. The larger the error, the larger the control signal. When the error is approximately zero or the response is close to the target, the control essentially does nothing. Assuming now that $K_p = 0$, the control signal simply becomes:

$$u(t) = K_I \int e dt \tag{4.32}$$

The addition of this integral makes the open-loop forward path of type 1. Thus, the system is guaranteed to have zero steady-state error to a step input. If *e* (*t*) is non-zero for any length of time (for example, positive), the control signal gets larger and large as time goes on. The integral term is an accumulation of the past values of the error. The PI control thus considers past and present values of the error in assigning its control value [32][35]. The integral gain is related to the proportional gain by:

$$K_i = K_p / \tau_i \tag{4.33}$$

Where, τ_i is the integral time constant.

Proportional action can reduce the steady-state error, but too much of it can cause the stability to deteriorate whereas the integral action is used to eliminate the steady-state error. Generally the PI control law is described as:

$$U^{PI} = K_p e + K_I \int e dt \tag{4.34}$$

$$U^{PI} = K_p (e + 1/\tau_i \int e dt) \tag{4.35}$$

where

U^{PI} is the control output, K_P is the proportional gain, K_I is integral gain, and e is the tracking error.

4.5.4 Fuzzy Logic based self tuning PI Controller

As we have seen in the above sections, to achieve a high performance speed control of PMSM Fuzzy Logic based self tuning PI Controller is proposed in speed loop of the control system. This collaboration is practical as most of the industrial system that are using conventional controller can insert a FLC to their control system for optimization purposes without changing much of the system topology and scrapping the conventional controller. As a result fuzzy logic controller (FLC) is used to aid conventional method to enhance the output performance by retuning the gains of PI controller at different operating conditions. As a result, the available conventional controllers that can do their job are never replaced by fuzzy logic controller to avoid adding unnecessarily cost to the system [5].

The accurate mathematical model is not necessary to Fuzzy Logic based tuning PI controller. The practical experience is saved in the form of control rules, then the correct control decision is made according to the practicable condition of control system(the magnitude, direction and the change trend of the input signal deviation).The parameters K_P, K_I can be adjusted on-line, So the control performance of PMSM servo system can be improved.

a. The input variables and output variables

The Fuzzy Logic-PI controller uses the speed error and error change rate as fuzzy inputs, and the proportional factor (K_{P1}) and integral factor (K_{I1}) as fuzzy outputs.

The error and rate of change of error are defined as:

$$e(k) = r(k) - y(k) \tag{4.36}$$

$$ce(k) = \frac{e(k) - e(k-1)}{T_s} \tag{4.37}$$

where

r(k) is the reference input speed signal, *y (k)* is the output speed response, *e(k)* is the error signal, and *ce(k)* is the rate of change of error.

Now the control action of the PI controller after self tuning can be describing as:

$$U(k) = K_{p2}e(k) + K_{I2}\sum_{i=0}^{k-1} e(i) \tag{4.38}$$

$$K_{p2} = K_{p1} * K_p \tag{4.39}$$

$$K_{I2} = K_{I1} * K_I \tag{4.40}$$

where

K_{p2}, and K_{I2} are the new gains of the PI Controller.

K_{P1}, K_{I1} are the gains outputs of fuzzy control that are varying online with the output of the system under control and K_P, K_I are the optimal values of the PI Controller before tuning.

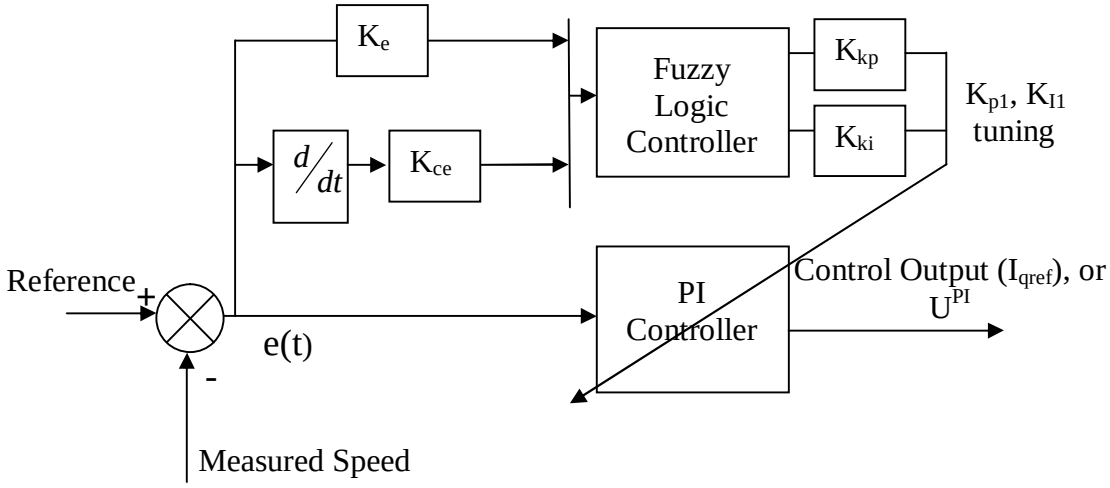

Figure 4.18: Structure of fuzzy logic based self tuning PI Controller.

b. Fuzzy language of input and output variables

The gains K_e, K_{ce}, K_{kp}, and K_{ki} in Figure 4.18 are called scaling factors used to obtain normalized inputs and outputs for the fuzzy logic controller. The use of normalized domains requires a scale transformation, which maps the physical values of the process input variables into a normalized domain. This is called input normalization. Furthermore; output denormalization maps the normalized value of the output variable (K_{p1} & K_{I1}) into its respective physical domain. For the system under study the universe of discourse for both inputs e(t) and ce(t) is normalized to the range -1 to 1 as the range of the universe of discourse for the membership functions is selected to be from -1 to 1, and the linguistic labels(fuzzy sets) are defined as{NB (Negative Big), NM(Negative medium), NS (Negative small), ZE (Zero), PS (Positive small), PM (Positive medium), and PB (Positive Big) } and are referred to in the rules bases as {NB,NM,NS,ZE,PS,PM,PB }as it is shown in Figure 4.19. The linguistic labels of the outputs K_{p1} and K_{I1} in the range 0 to 1 are {Zero, Medium small, Small, Medium, Big, Medium big, very big} and referred to in the rule bases as {Z, MS, S, M, B, MB, VB}. The membership functions of the inputs fuzzy sets and output fuzzy sets are shown in Figure 4.19 and 4.20. These membership functions are chosen based on intuition, simply derived from the capacity of humans to develop membership functions through their own understanding.

The precise shapes of the membership function curves are not so important in their utility. Rather, it is the approximate placement of the curves on the universe of discourse, the number of membership functions used, and the overlapping characteristics are the most important[5][34].

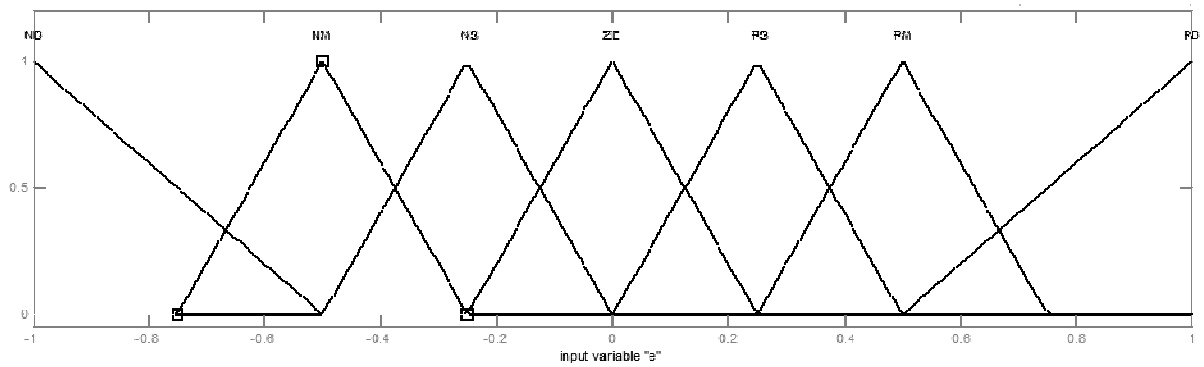

Figure 4.19: Member ship functions of inputs (e, Δe).

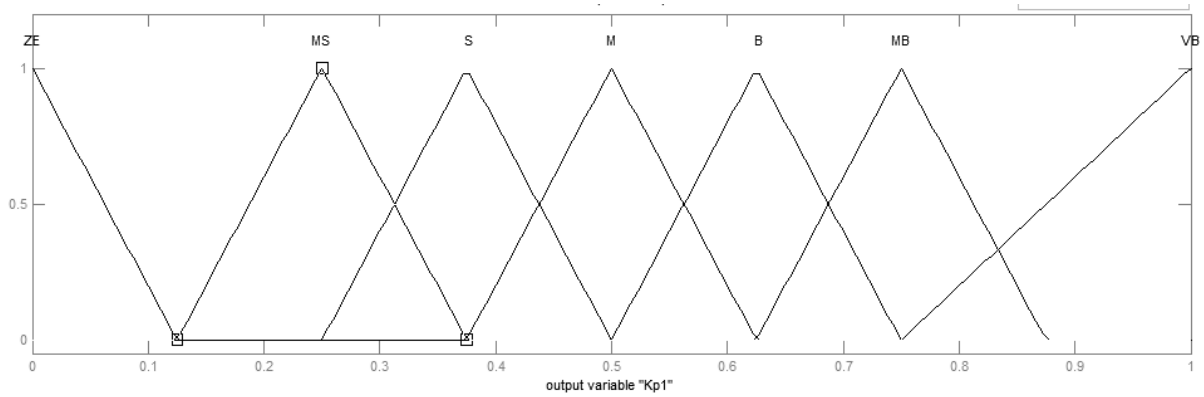

Figure 4.20: Member ship functions of outputs (K_{P1}, K_{I1}).

C. Fuzzy rules

The principle of designing fuzzy rules is that the output of controller can make the PMSM drive system output response dynamic and static performance optimal. Formulation of the fuzzy rules is according to the simulation analysis of the PMSM drive system. The rule base is expressed as IF (antecedent)-THEN (consequent) rules shown in equation (4.41).

IF e(t) is NB and ce(t) is NB THEN K_{p1} and K_{I1} are ZE (4.41)

where

NB is the linguistic label of input, and ZE is the linguistic label of output.

Tables (4.4) shows the control rules for determining K_{P1} and K_{I1}that are used to tune the PI controller gains in the FL-PI controller.

Table 4.4: Rule bases for determining the gains K_{P1} and K_{I1}.

ce\e	NB	NM	NS	ZE	PS	PM	PB
NB	ZE	ZE	MS	MS	S	S	M
NM	ZE	MS	MS	S	S	M	B
NS	MS	MS	S	S	M	B	B
ZE	MS	S	S	M	B	B	MB
PS	S	S	M	B	B	MB	MB
PM	S	M	B	B	MB	MB	VB
PB	M	B	B	MB	MB	VB	VB

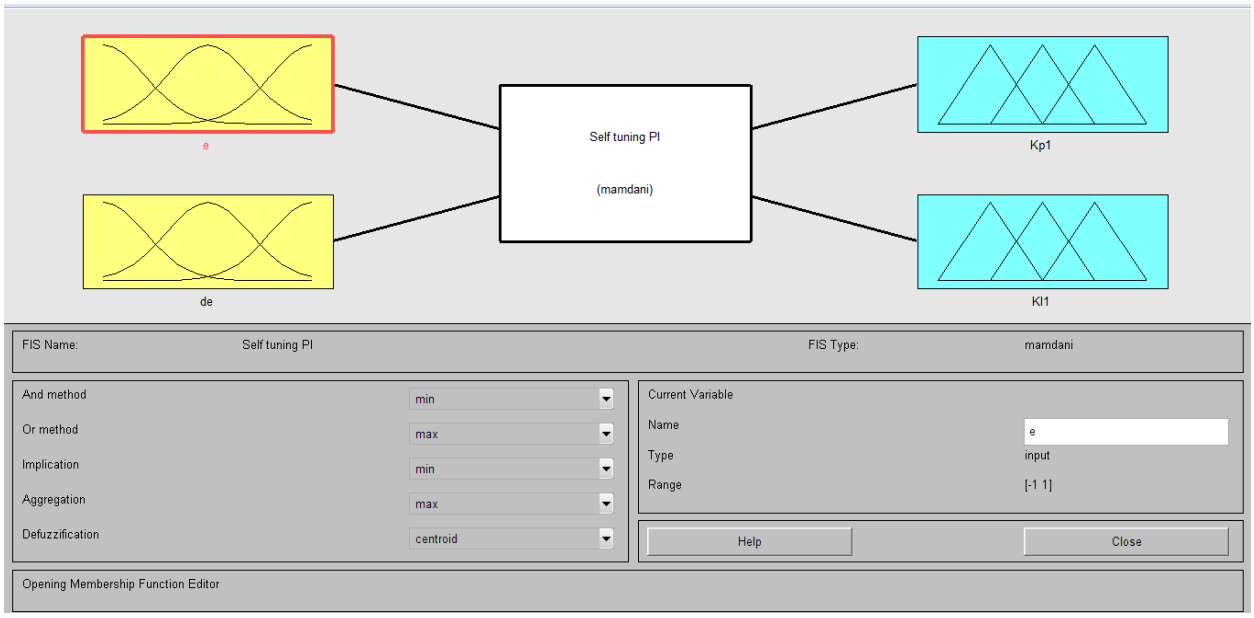

Figure 4.21: Fuzzy inference block.

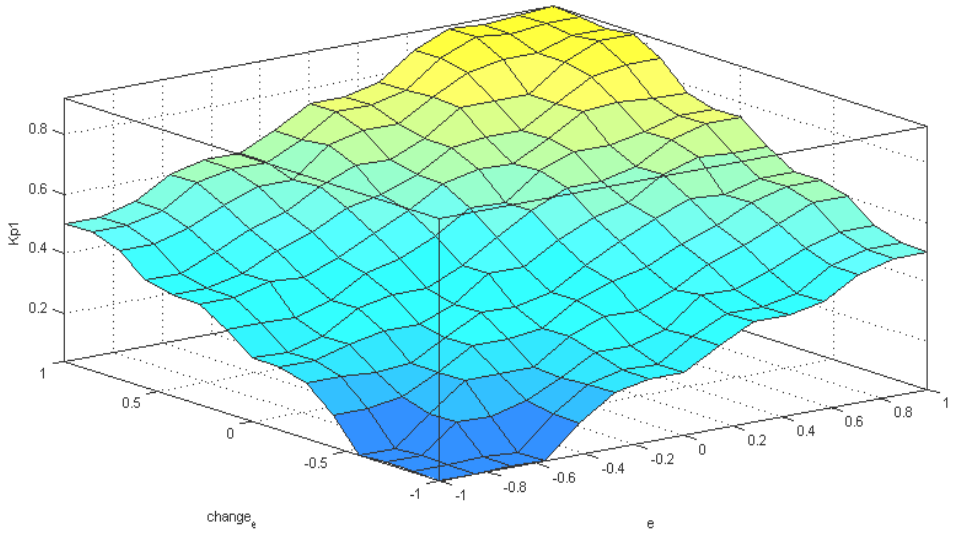

Figure 4.22: Variation of K_{p1} and $K_{I1}$with respect to error and change in error of speed.

4.5.5 Design of Current Controller

4.5.5.1 Introduction

For decoupled torque and flux control the rotor flux and torque current have to be properly controlled, which makes current regulator very important part of the field oriented based control system In order to design the regulator the existing delays in the system need to be taken into account. These delays in the case of a motor drive are due to the digital implementation of the control (which implies the sampling of signals), the use of filters, the processing of the control algorithm and the use of Pulse Width Modulators (PWM).

4.5.5.2 i_q's PI controller design

For the design of PI-controllers it is necessary to know the closed loop transfer function. Using the q-axis voltage equation, torque equation, and Mechanical equation, The Block diagram of permanent magnet synchronous motor (PMSM) in *q*-axis is shown in Figure 4.23.

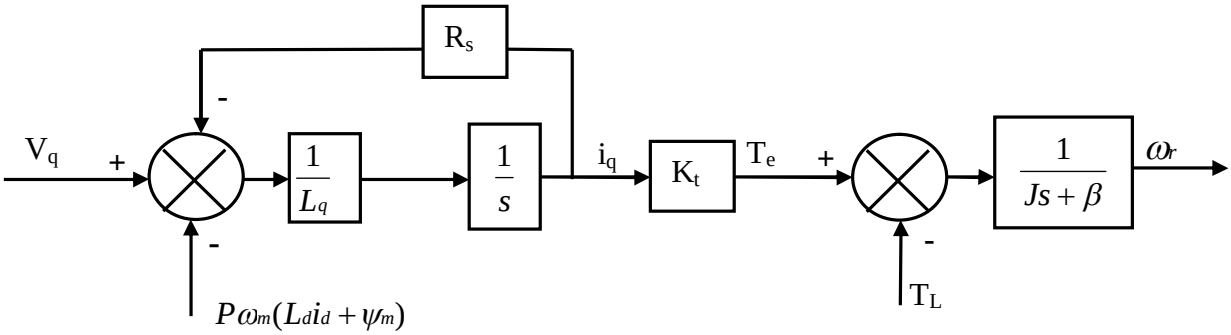

Figure 4.23: Block diagram of PMSM in q-axis.

Here, the design objective is to determine the PI's gains K_p and K_i (or T_i) so as to achieve a good closed loop response. The transfer function between torque component, i_q and input voltage, V_q in *q*-axis is:

$$\frac{i_q}{V_q} = \frac{1/R_s}{\tau_e S + 1} \tag{4.42}$$

For the design of PI-controller of current loop in *q*-axis, the block diagram in Figure 4.24 is used.

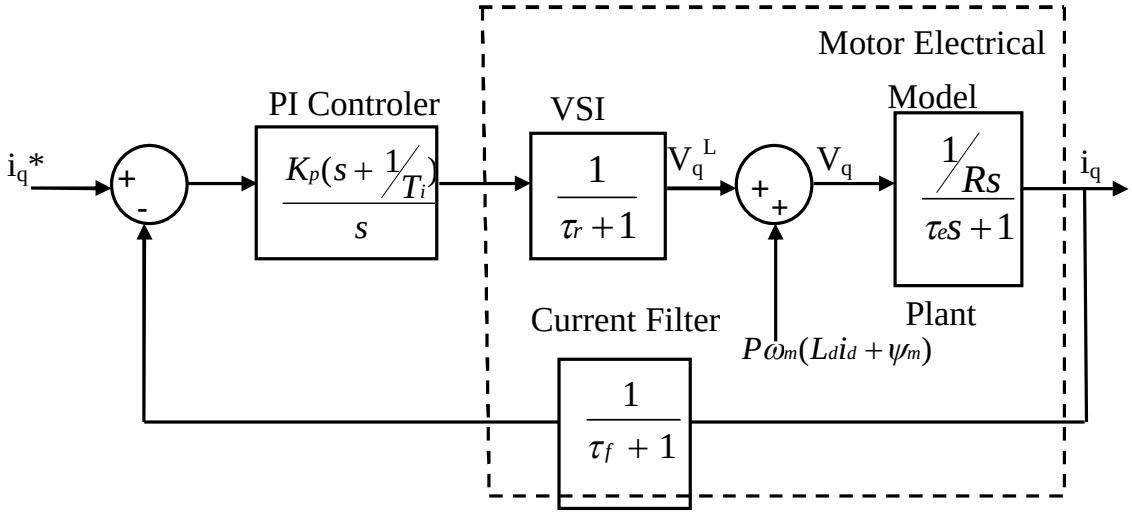

Figure 4.24: Block diagram of q-axis Current loop.

where

τ_r is the inverter time constant which is given by or it is the delay before the demand voltage (V_q) appears on the motor lines

T_{sp} is PWM sampling period

τ_e (electrical time constant) =L_s/R_s and τ_f is current filter time constant

K_p, T_i are the proportional gain and Integral time constant of the PI controller

Since the delays associated with the inverter and filter are very small when compared to current time constant (L_s/R_s) their dominance on the performance is small and can be neglected. As the result the controller block diagram can be simplified as shown in Figure 4.25.

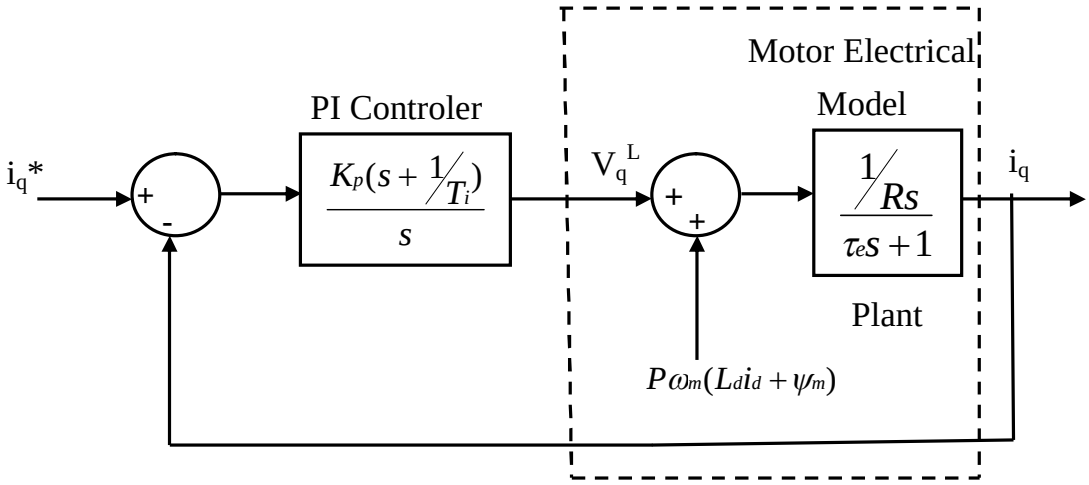

Figure 4.25: A simplified i_q's loop for PI controller design.

Design specification

Peak overshoot(MP)=20%, rise time(t_r) =0.0012sec =10T_s

where, T_s is sampling time of the current (inner)loop = 12μs.

From the design specification the damping coefficient (ζ) and un damped natural frequency (ω_n) are assigned as in equation (4.43).

ζ>=0.48, ω_n >=1500 rad/sec (4.43)

Using equation (4.43) the damping coefficient and natural frequency are chosen to be:

ζ=0.7 and ω_n =1500 rad/sec (4.44)

From Figure 4.25 the overall transfer function between the torque component i_q and its reference i_q* is as:

$$\frac{i_q}{i_q^*} = \frac{K_p(T_i s + 1)}{T_i L_q s^2 + T_i(R_s + K_p)s + K_p} \quad (4.45)$$

Comparing the 2nd order closed loop system performance in equation (4.46) with equation (4.45), the values of K_p &T_i in terms of the motor parameters in Table B1(Appendix B) are found in equation (4.47).

$$\frac{\omega_n^2}{s^2 + 2\xi\omega_n s + \omega_n^2} \quad (4.46)$$

$$K_p = 2\varsigma\omega_n L_q - R_s$$
$$T_i = \frac{K_p}{\omega_n^2 L_q} \tag{4.47}$$

4.5.5.3 i_d's PI controller design

Using the d-axis stator voltage equation the block diagram of permanent magnet synchronous motor (PMSM) in *d*-axis is shown in Figure 4.26.

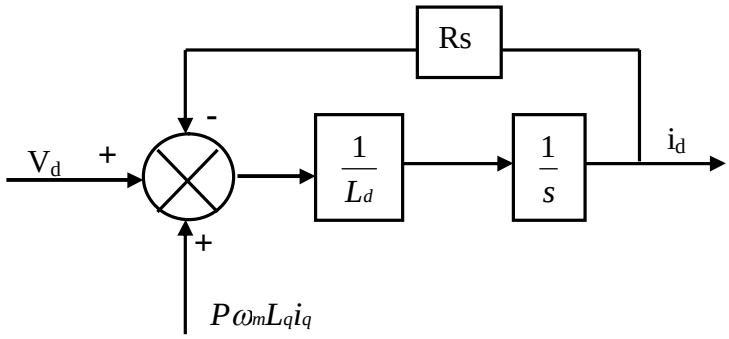

Figure 4.26: Block diagram of PMSM in d-axis.

The transfer function between flux component, i_d and input voltage, V_d in *d*-axis stator current is given by equation (4.48).

$$\frac{i_d}{V_d} = \frac{1/R_s}{\tau_e S + 1} \tag{4.48}$$

In the constant torque operation region of PMSM due to the presence of the constant flux of the permanent magnet, there is no need to generate flux by means of the i_d current, i.e. i_d=0, which decreases the stator current and increases the efficiency of the drive. In order to design the PI current regulator in *d* axis it is followed the same procedure as q axis and K_p and T_i are the same as equation(4.47) since L_q=L_d in surface Permanent Magnet Synchronous Motor (SPMSM).

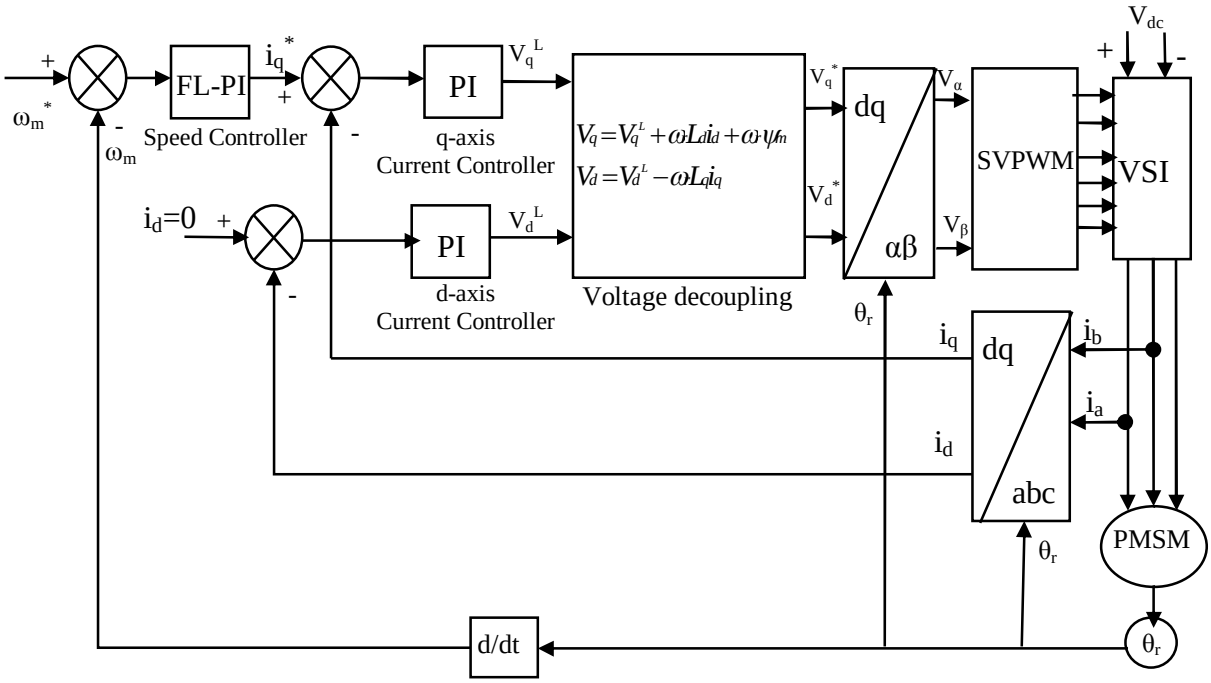

Figure 4.27: The overall PMSM Control Structure.

CHAPTER FIVE
SIMULATION RESULTS AND DISCUSSIONS

This chapter of the thesis is concerned with the simulation results of the closed loop control of the system using Fuzzy-Logic with Matlab/Simulink. In the simulation part only the operation below the base speed will be explained. SIMULINK® is a toolbox extension of the MATLAB program. It is a program for simulating dynamic systems. Simulink has the advantages of being capable of complex dynamic system simulations, graphical environment with visual real time programming and broad selection of tool boxes. Its graphical interface allows selection of functional blocks, their placement on a worksheet, selection of their functional parameters interactively, and description of signal flow by connecting their data lines using a mouse device. Simulink simulates analogue systems and discrete digital systems. It is also gives the opportunity to transform other programming language and .m files of Matlab in to a block to use in the Simulink environment. This is achieved by transforming the codes into s-function, which is .m file of Matlab.

The motor control algorithm is developed for Texas Instruments™ C2000™ DSP with Target Support Package™ TC2. In addition to the simulation an attempt is made to formulating software that will be used to simulate in the F2812 device simulator.

5.1 Simulation of the drive system

This section deals with the simulation results of PMSM drive system using the motor parameters in Table B1 of Appendix B. The system built in Simulink for a PMSM drive system has been tested at the constant torque regions of operation.

5.1.1 Simulink model of PMSM Drive system

The overall Matlab/Simulink model of the PMSM drive and Control system is shown in Figure 5.1. All the components of the real drive system are modeled to study the simulation result.

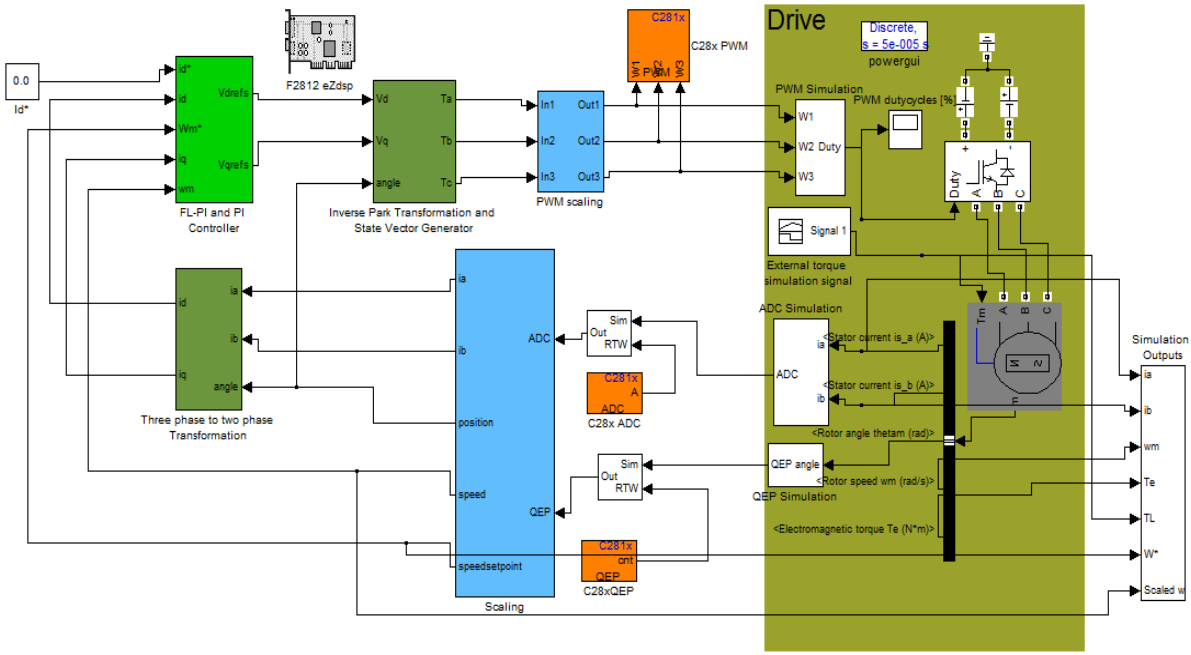

Figure 5.1: Matlab/Simulink Model of the PMSM drive.

Figure 5.2: shows the block diagram of Fuzzy Logic-PI Controller for speed and PI Controller for current of PMSM drive system, which is the Simulink block implementation of Figure 4.27.

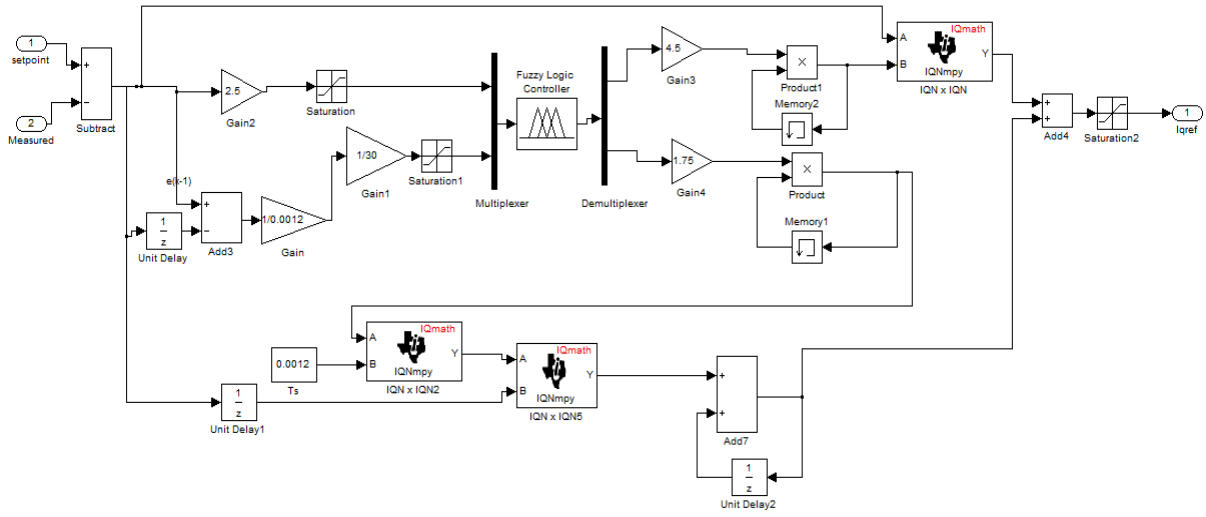

Figure 5.2: The Matlab/Simulink model of Fuzzy Logic-PI Speed Control structure.

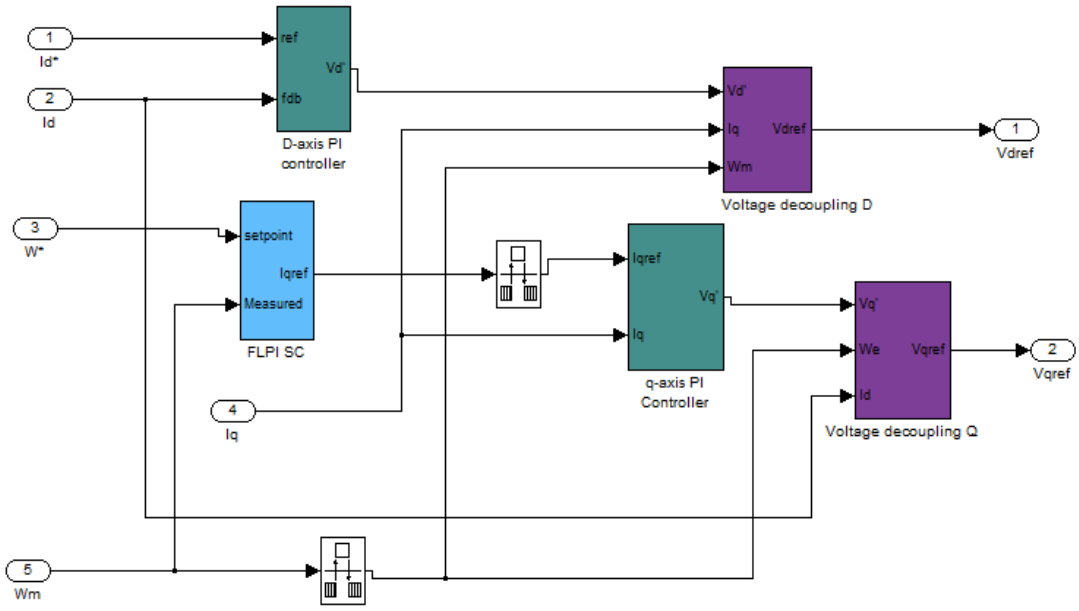

Figure 5.3: The overall speed and current controller in Matlab/Simulink.

5.1.2 The IQmath and DMC libraries

The two libraries included in the Target for TI C2000 package for developing embedded control system are the IQmath and the DMC (Digital Motor Control) library. The blocks in these libraries correspond to functions in the TI C28x IQmath and DMC assembly code library which are written to optimize the processors in the C2000 family.

a. IQmath library

Texas Instruments TMS320C28x IQmath Library is collection of highly optimized and high precision mathematical functions for C/C++ programmers to seamlessly port a floating-point algorithm into fixed point code on TMS320C28x devices. These routines are typically used in computationally intensive real-time applications where optimal execution speed and high accuracy is critical. By using these routines you can achieve execution speeds considerable faster than equivalent code written in standard ANSI C language. In addition, by providing ready to- use high precision functions, TI IQmath library can shorten significantly your DSP application development time. Some of the blocks used for the implementation are fixed point

multiplier, fixed point integrator and differentiator, data type transformers, and data type convertor.

b. DMC library

To use a digital controller for motor control, the system needs a little more computing power. Like the IQmath libraries, the blocks in the DMC library are also efficient for digital motor controller implementation. The function that are implemented by the blocks in these libraries are for example Clark and Park transformations, a space vector generator, ramp control, and ramp generator. This implies that the code generated from blocks in these libraries is very efficient and optimized in comparison to writing algorithm that substitutes the blocks in these libraries. The blocks in these libraries can also be used in simulink simulation together with some of the basic Simulink blocks. In general all input and output signals for the IQmath and DMC blocks are fixed point numbers.

5.1.3 Software Organization

Overall algorithm of simulation is divided into two: initialization and running the model. The initialization step defines and initializes the control parameters and constants while the second step is running the model. Discrete simulation has been carried out for the implementation of the drive using Matlab/Simulink. The following flow chart is followed to investigate the control of PMSM over a constant torque operation region.

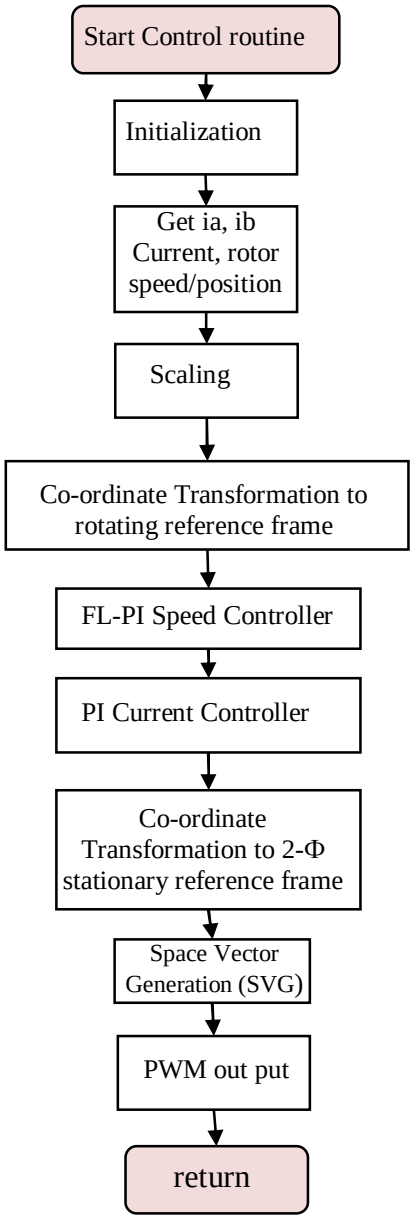

Figure 5.4: Flow chart of the system.

5.1.4 Simulation Results

The overall Matlab/Simulink model of the PMSM drive allows simulating the behavior of the machine using sensored feedback and Fuzzy Logic-PI algorithm for different operating modes. First, response of the system is tested for step speed input and the speed response for consecutive step levels is tested. Second, the impact of machine speed response for torque

variation is simulated. Then, the effect of parameters variation (moment of inertia and friction coefficient) on the speed response is simulated and is compared to the speed response using the PI Controller. Figure 5.5: shows the speed response of the motor when the motor is commanded at a reference speed of 100rad/sec.

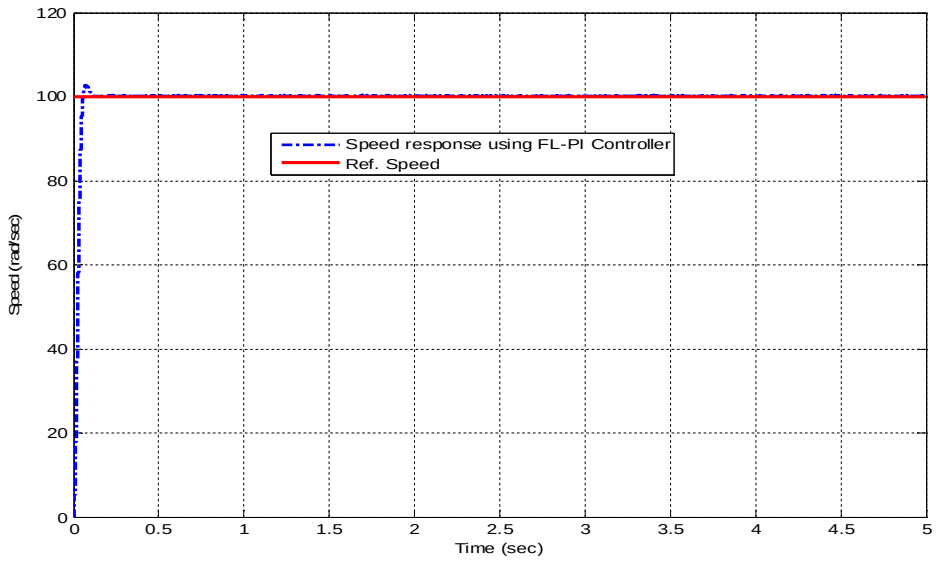

Figure 5.5: Speed response of the machine for 100rad/sec reference speed.

Figure 5.6 shows the developed electromagnetic torque. The starting torque until 0.03 sec is around 2.5 Nm which is due to primarily the acceleration of the rotor to reach to the steady speed of 100 rad/sec. The starting torque is higher when compare to the steady state value. So this generated torque is meant to support acceleration of the rotor and the friction retard without the load torque (T_L=0). However, after 0.03sec the generated torque is reduced almost to 0 Nm to support only the approximately zero retard friction.

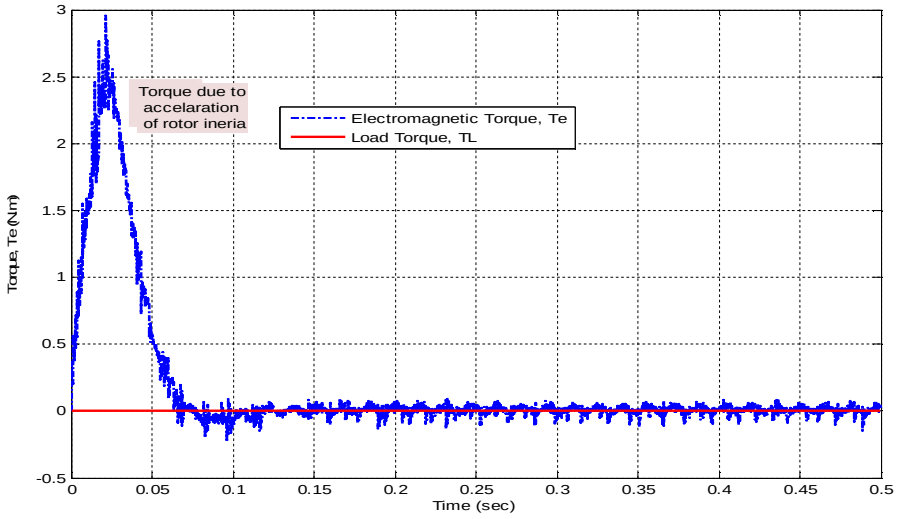

Figure 5.6: Developed electromagnetic torque for a step speed input.

It is clear that the current is non sinusoidal at the starting and becomes sinusoidal when the motor reaches the controller command speed at steady state. Figure 5.7 shows the two phase currents (i_a and i_b) drawn by the motor when the motor is operating at a reference speed.

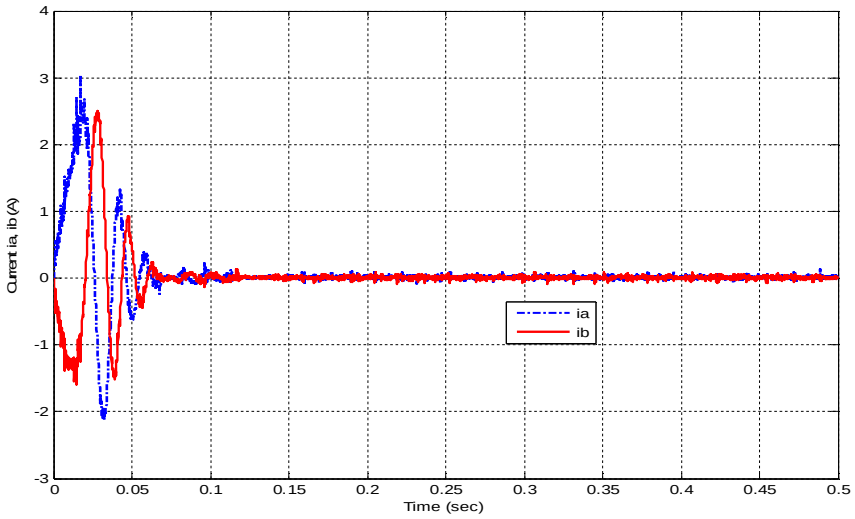

Figure 5.7: i_a & i_b Currents as motor accelerating to 100 rad/sec speed input.

Figure 5.8 shows the speed response of the Motor for 100 rad.sec reference speed input for PI controller and FL-PI controller.

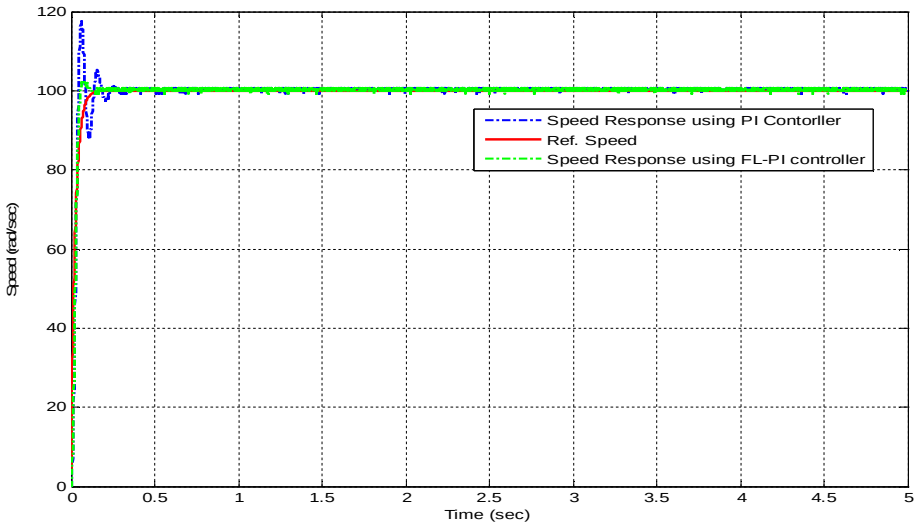

Figure 5.8: Speed response of PI and FL-PI Controller for 100 rad/sec reference speed input.

Figure 5.9 shows the speed response of the machine for two ramped step speed level desires. First the speed desire is set to be 100rad/sec. Then the speed changes instantly at t = 0.5s and attains it steady speed of 160 rad/sec. Figure 5.10 shows the speed response for two ramp speed level commands and Figure 5.11 shows the current drawn by the machine for the two ramped step speed level command.

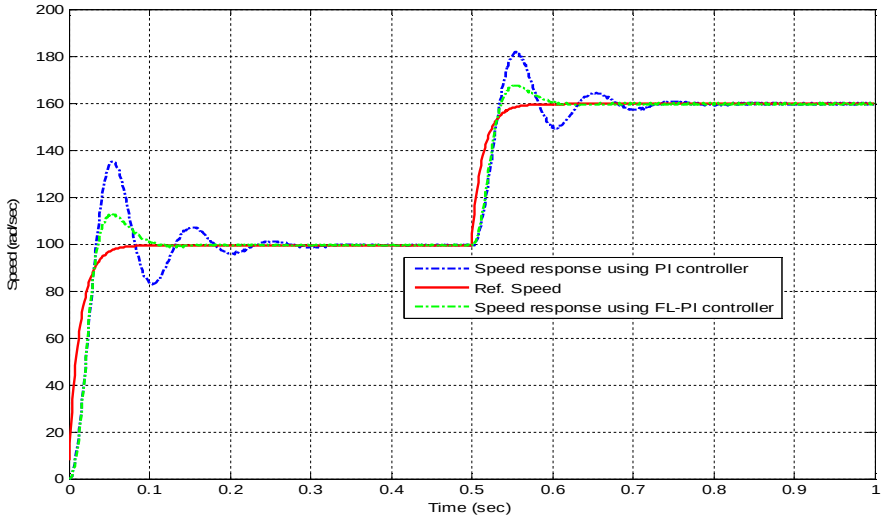

Figure 5.9: Reference speed and speed response at two ramped step speed levels.

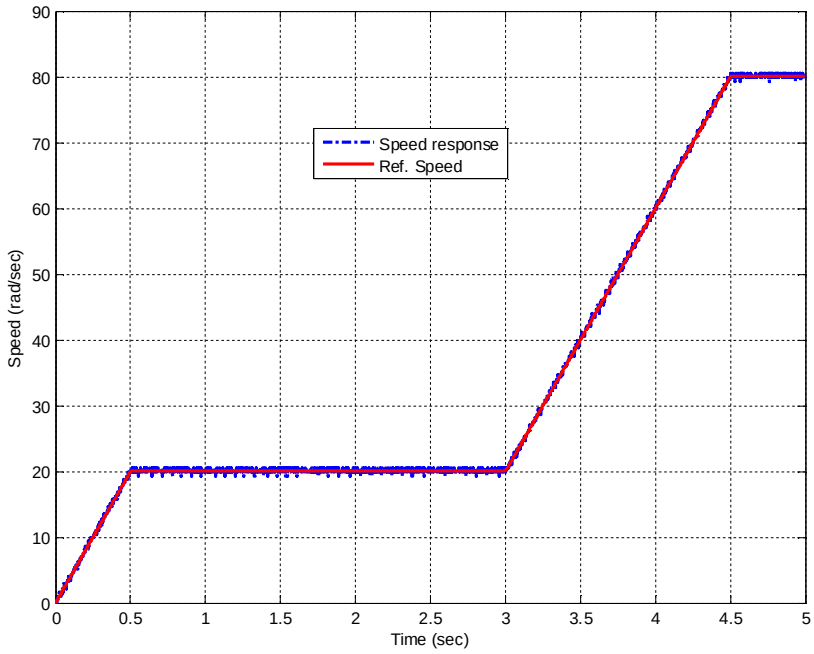

Figure 5.10: Reference speed and speed response for two ramp speed levels.

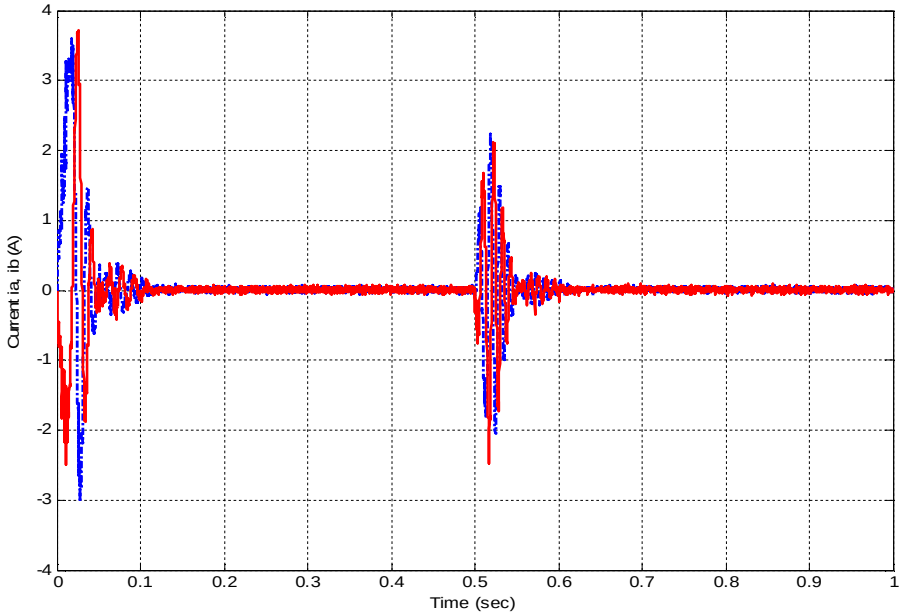

Figure 5.11: Current drawn by the motor for two level speed commands.

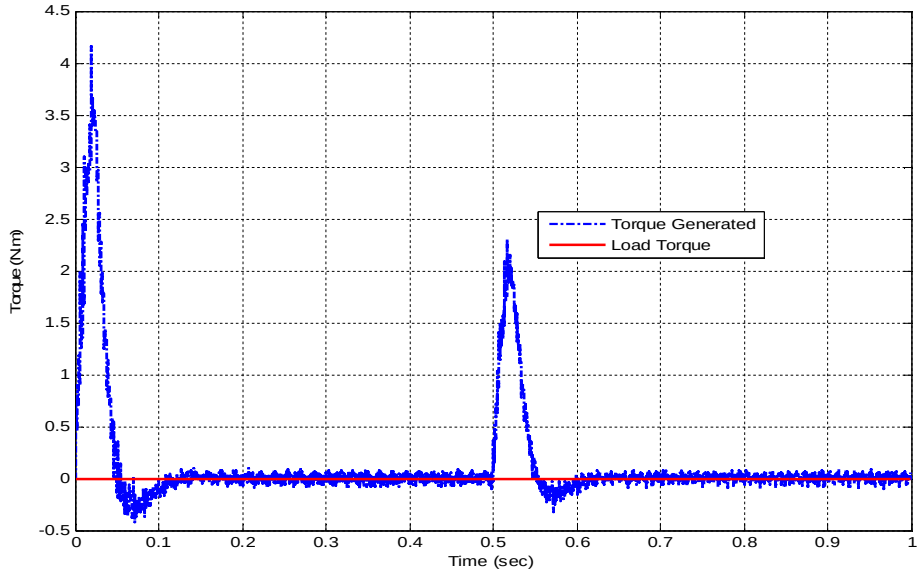

Figure 5.12: Electromagnetic torque generated for the two step level speed input.

Figure 5.13 presents the speed response of the system when motor moment of inertia is increased by 50% of the nominal value and Figure 5.14 presents the speed response of the system when motor friction coefficient is increased by 50% of the nominal value without load torque. As it is shown from Figure 5.13 and 5.14 the performance of the controller decreases to some extent i.e. peak overshoot increases, settling time increases, and rise time is decreased.

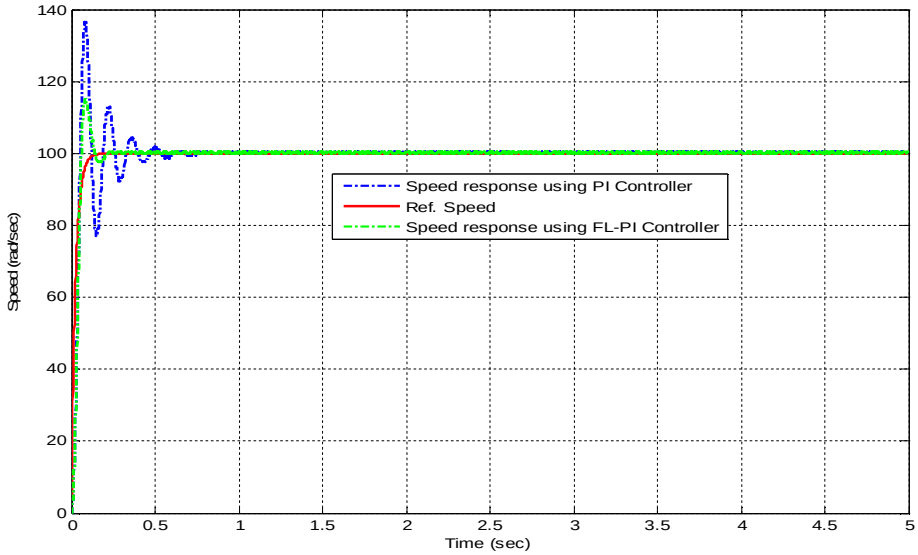

Figure 5.13: Speed response when moment of inertia is increased by 50%.

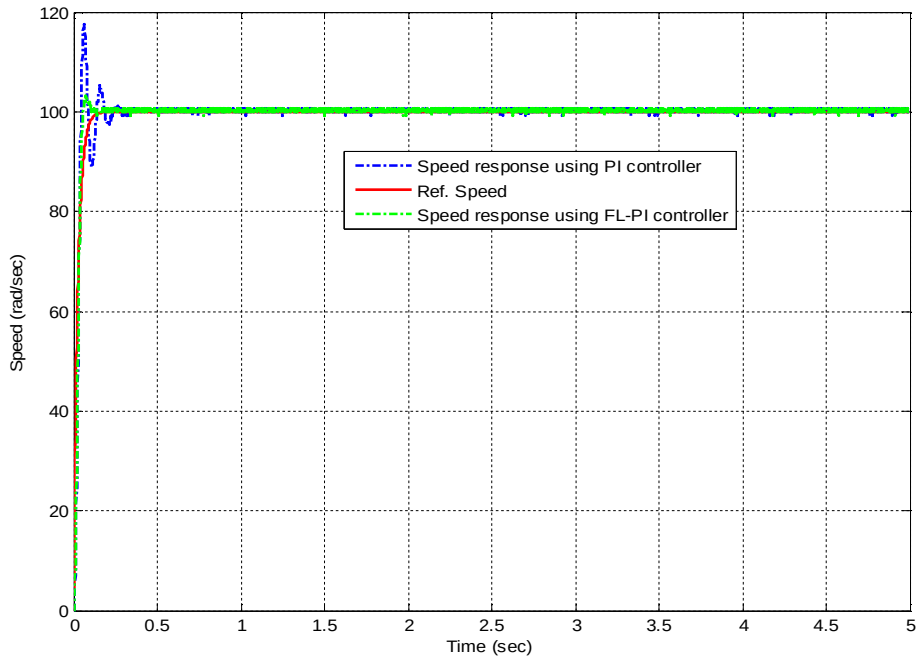

Figure 5.14: Speed response when friction coefficient is increased by 50%.

Figure 5.15 and 5.16 illustrates the speed and torque response of the system in load torque variation. The drive system is started at no load torque and a constant load of 3N.m applied at t=0.5s, again a zero load torque is applied at t=1s, and a step load torque of -3N.m is applied at t = 1.5s. The speed response of the machine in the variation of the load torque applying Fuzzy Logic based tuning PI and PI controller is shown under Figure 5.15. As the figure illustrates, at t= 0.5 the speed would decrease while a positive external load torque applied, and vice versa at t=1.5. It shows that PI controller cannot obtain a rapid recovery of the external load disturbance. Figure 5.16 depicts the torque generation for the application of the load torque. Figure 5.17 shows current drawn by the motor for the load disturbance explained above.

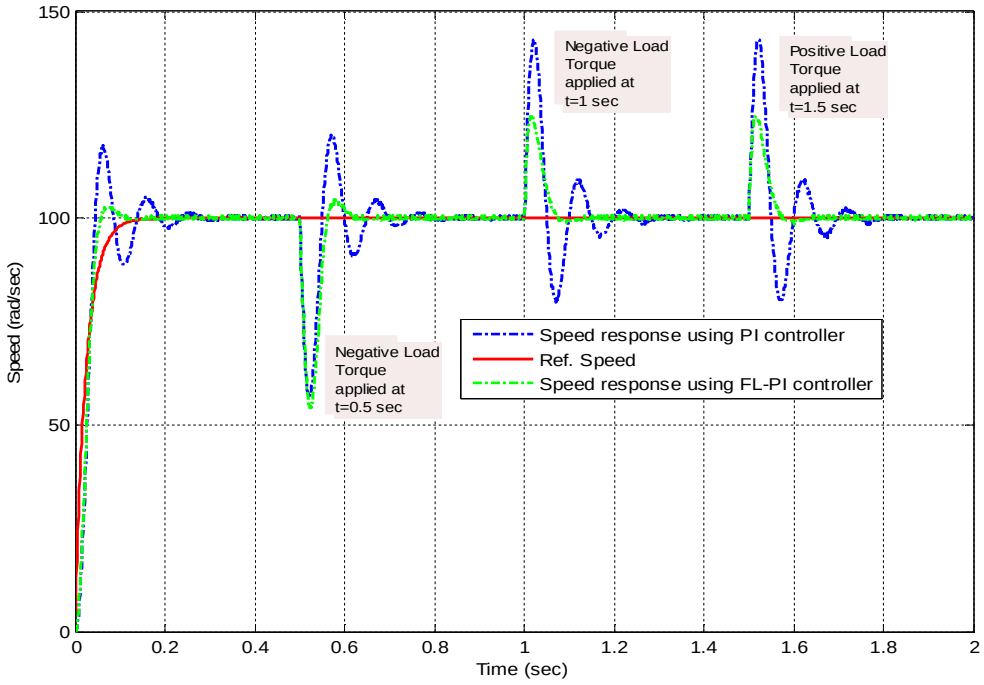

Figure 5.15: Speed response in load torque variation.

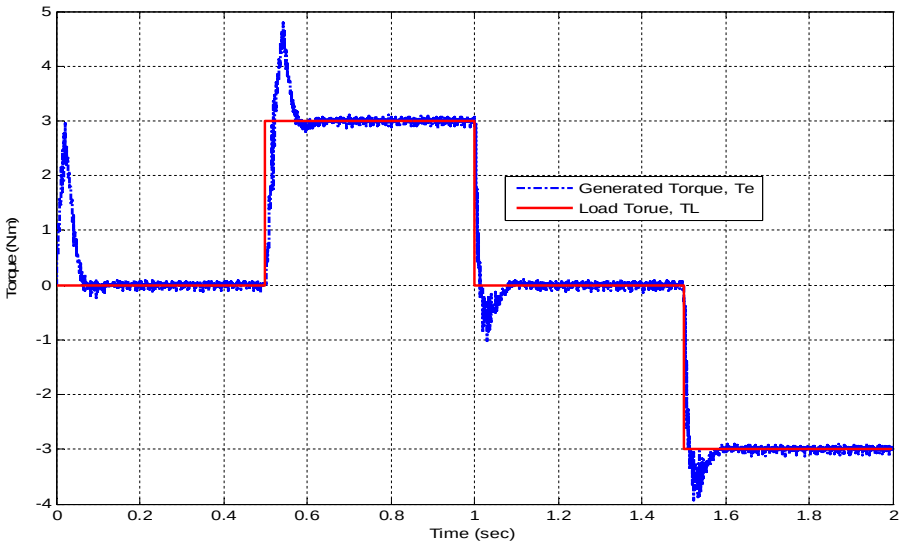

Figure 5.16: The Electromagnetic Torque generated and load torque.

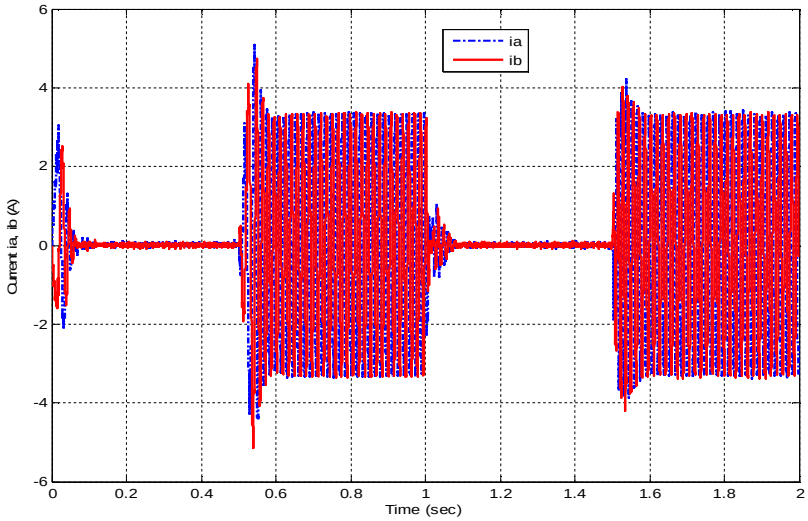

Figure 5.17: Two of the three phase currents of the machine in load torque variation.

5.1.5 Stability and Performance evaluation of the FL-PI Controller

a. Stability and Performance evaluation by observing the response

Stability and performance evaluation of FLC is studied by observing the response curve of the system. The response curve shows the dynamics of the system responding to changes in its inputs. A small set of standard signals like unit step, and unit ramp are studied. If a system responds well to these signals, a control engineer judges it as a good system. In control theory there are many methods to analyze the system stability such as Nyquist's stability criteria, Routh's stability criteria, describing function approach, and phase plane method. Unfortunately these methods cannot be used for stability analysis of fuzzy control systems all of them require a special mathematical model of a control system prior to stability analysis [4].

b. Stability and performance indicators

The stability and performance is evaluated by observing the system responses in the above simulation results and its parameters like overshoot, rise time, settling time, and steady state error (ess). The simulation results show that the FL-PI controller have shorter regulating time, and fast recovery from speed changes and load disturbance. As it is shown from the results the designed FL-PI controller is stable.

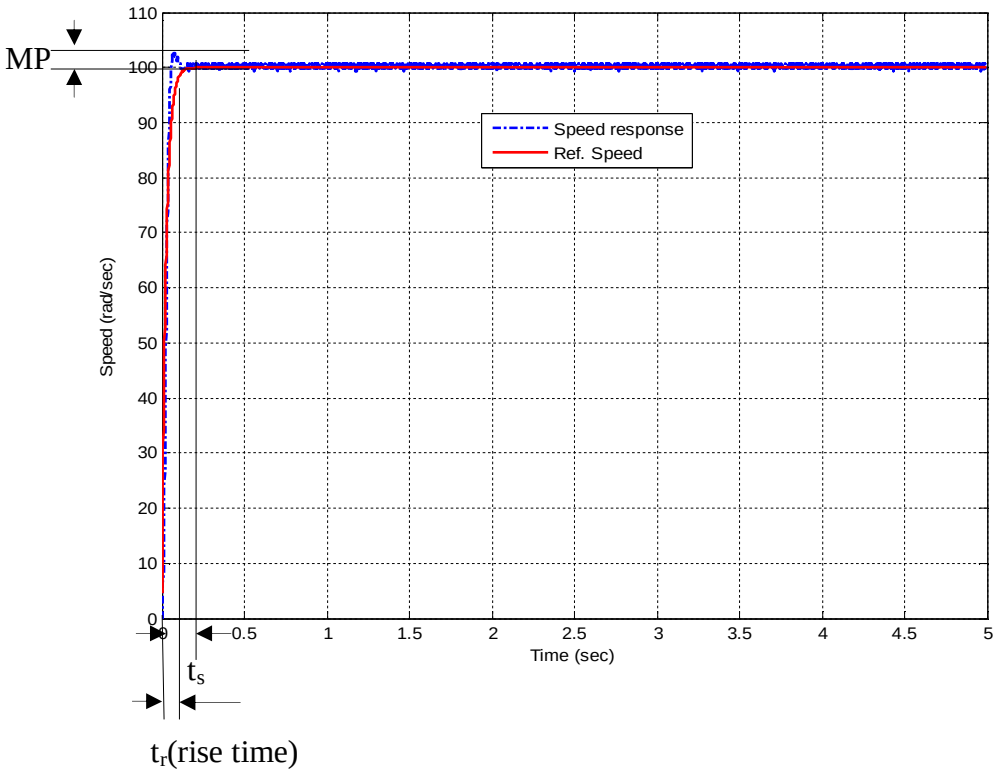

Figure 5.18: The FL-PI Controller Performance parameters.

Table 5.1: Performance Comparison of FL-PI and PI Controllers.

NO.	Performance parameters	PI	FL-PI
1	Overshoot(MP) at 100 rad/sec, no load torque applied	17.5%	2.5%
2	Settling time(t_s) at 100 rad/sec, no load torque applied	0.366 sec	0.1692 sec
3	Overshoot at 100 rad/sec, 3 N.m Load torque applied	35%	17%
4	Settling time at 100 rad/sec, 3 N.m Load torque applied	0.4224 sec	0.1824 sec

5.2 DSP based controller

With the rapid development in microprocessor, the high performance digital signal processor (DSP) has become a popular area of research in the field of the digital control for ac drives due to their high-speed performance, simpler circuitary, on-chip peripherals of a micro-

controller into a single chip solution. Especially, the new generation DSP controller TMS320F2812 produced by Texas Instrument, which provides the advantages of high speed (150MIPS), up to 128Kx16 flash, two sets (total 12 lines) of PWM outputs, two sets (total 6 lines) of QEP inputs, a 16-channels 12-bit A/D converter (200ns conversion time) and a 56-bits GPIO is very suitable to develop a fully digital controller and a complicated intelligent control algorithm in AC motor drives[22][29].

5.2.1 F2812 Device Simulator

F2812 Device Simulator simulates the TMS320F2812 digital signal processor in Matlab/Simulink after code generation using processor in the loop method. The simulator checks weather the controller algorithm works or not on the real DSP.

5.2.2 Code Composer Studio

Code Composer Studio (CCS) is the standard Integrated Development Environment (IDE) for all families of DSPs. It provides an interface between Matlab and TI DSPs. Code Composer Studio allows projects to be designed and tested using Simulink, generate code for Texas Instrument (TI) DSPs directly from the model, and evaluate their performances and optimized. The c-code of the Matlab/Simulink model of PMSM drive is generated using an application suite Real Time Workshop (RTW) embedded coder and Code Composer Studio. The following versions of the application suites are used for this thesis.

- Real-Time workshop Embedded Coder v5.2
- Code Composer Studio v3.3
- Embedded IDE Link to Code Composer Studio v3.3

The relationship between Matlab, Code Composer Studio, and a Texas Instruments DSP is shown in Figure 5.19.

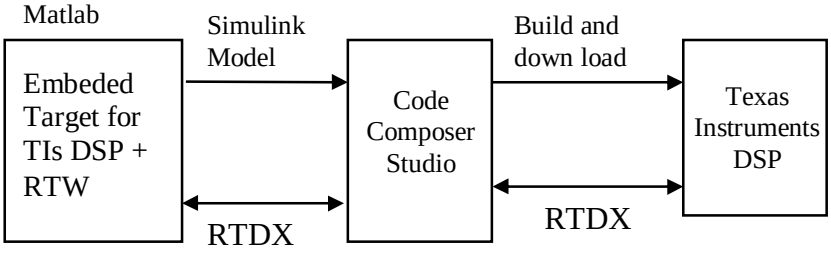

Figure 5.19: The relationship diagram of Matlab, CCS, and TI DSPs.

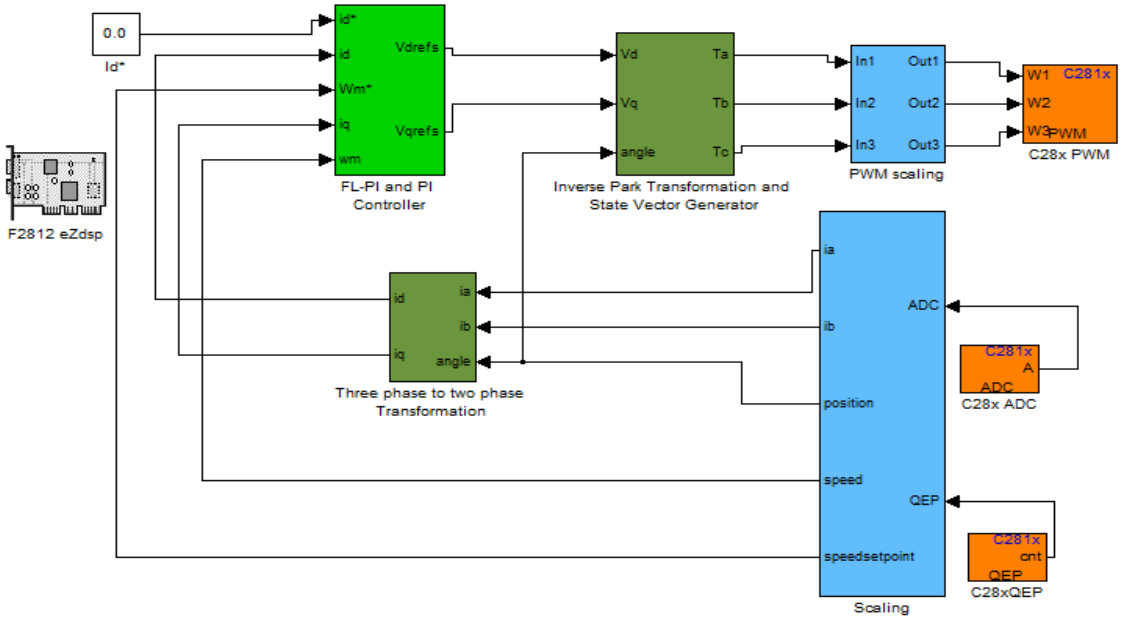

Figure 5.20: Implementation model built using TI C2000 Toolbox.

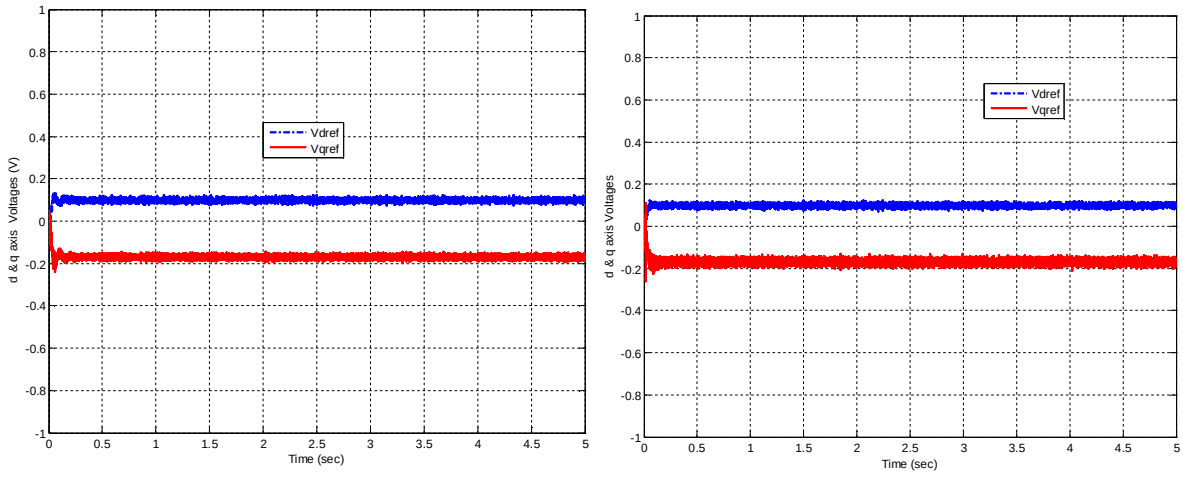

Figure 5.21: a) The output control Voltages V_{dref} and V_{qref} of the Controller in Simulink model. b) The output control voltages V_{dref} and V_{qref} of the Controller from the F2812 Device Simulator.

CHAPTER SIX
CONCLUSIONS AND RECOMMENDATIONS

6.1 Conclusions

The thesis presented a complete review of the Permanent Magnet Synchronous Machines. The PMSM servo system is a nonlinear and time-varying complex system. The results of traditional PI controller as speed control of PMSM are not satisfactory to the higher degree of accuracy condition. The fuzzy control not only has the prominent advantage In complex, time-varying and nonlinear system control but also don't need the mathematical model of controlled object.

A self-tuning fuzzy logic controller (FLC) that tunes the gains of PI controller was developed according to the PMSM drive system characteristic, which has the advantages of PI control and fuzzy control. The controller is used as the speed controller in PMSM control system, which can adjust the PI controller parameters on-line according to the speed error and the speed error change rate.

The complete system has been simulated using the software package Matlab/Simulink. The simulation encompasses the entire system: the controller, the inverter, and the machine. Simulation results for system are presented in the fifth chapter. Three modes of operation are investigated: the behavior with a load torque variation at a constant speed, the performance with a speed change for a constant load torque, and speed response for friction coefficient and moment of inertia variation.

The simulation results show that fuzzy logic based self tuning PI controller have improvements in terms of zero steady-state error, small settling time, low overshoot, and fast recovery from load changes and parameter variations compared to the traditional PI controller with fixed gains. Since, PI controller is still widely used in industry; the developed FLC can be applied to the available PI controller for optimization purposes once the implementation is carried out successfully.

After the simulation phase, stability analysis of the results using some performance parameters, and generating the c-code of Matlab/Simulink model of the controller through code composer studio is presented. The different software packages necessary for the automatic code generation are also explained.

6.2 Recommendations

The main recommendations for this thesis are summarized as:

- ✓ If all equipments are available, the developed fuzzy logic based tuning PI speed controller can be implemented for sensor based PMSM control using the DSP board
- ✓ Sensorless control can also be (with no rotor position sensor) implemented.
- ✓ The thesis can also extend to operate the motor in the speed region beyond the rated speed; in field weakening region. A flux-weakening technique is applied when extension of the motor speed beyond base speed is desired.

REFERENCES

[1] R. Krishnan, "*Permanent Magnet Synchronous and Brushless DC Motor Drives*", Electrical and Computer Engineering Department, Virginia Tech Blacksburg, Virginia, U.S.A., CRC Press Taylor & Francis Group, 2010.

[2] R. Krishnan, "*Electric Motor Drives Modeling, Analysis, and Control*" Virginia Tech Blacksburg, Virginia, U.S.A., 2001.

[3] BIMAL K. Bose, "*Modern Power Electronic and AC Drives*" The University of Tennessee, Knoxville, Upper Saddle River, NJ07458, 2001

[4] LEONID REZNIK, "*Fuzzy Controllers*" Victoria University of Technology, Melbourne, Australia, Reed Elsevier plc group, 1997

[5] Mutasim Nour (Corresponding author), Omrane Bouketir & Ch'ng Eng Yong, "*Self-Tuning of PI Speed Controller Gains Using Fuzzy Logic Controller*" Modern Applied Science, November 2008, PP 55-65

[6] Yanpeng Dou, Zhang Ze, "*Design and realization of fuzzy self-tuning PID speed controller based on TMS320F2812 DSPs*" International Conference on Mechatronics and Automation, August 5 - 8, 2007, PP 3316-3320

[7] Rajesh Kumar, R. A. Gupta, Bhim Singh, "*Intelligent Tuned PID Controllers for PMSM Drive - A Critical Analysis*" Department of Electrical Engineering, Malaviya National Institute of Technology, Jaipur-3020 17, INDIA, Department of Electrical Engineering, Indian Institute of Technology, Delhi-110016, INDIA, 2006, PP 2055-2060

[8] Limei Wang, Mingxiu Tian and Yanping Gao, "*Fuzzy Self-adapting PID Control of PMSM Servo System*" School of Electrical Engineering, Shenyang University of Technology, Shengyang, China, 2007, PP 860-863

[9] B. Zigmund, A. Terlizzi, X. T. Garcia, R. Pavlanin, L. Salvatore, "*Experimental Evaluation of PI Tuning Techniques for Field Oriented Control of Permanent Magnet Synchronous Motors*" Advances in Electrical and Electronic Engineering PP 114-119

[10] A. Lidozzi, L. Solero, F. Crescimbini, A. Di Napoli, "*Direct Tuning Strategy for Speed Controlled PMSM Drives*" University ROMA TRE, Dept. of Mechanical and Industrial Engineering, 2010, PP1265-1270

[11] Zhen-Yu Zhao, Masayoshi Tomizuka, and Satoru Isaka, "*Fuzzy Gain Scheduling of PID controllers*" IEEE TRANSACTIONS ON SYSTEMS. MAN, AND CYBERNETICS., 1993, pp 1392-1398

[12] Shin-Hung Chang, Pin-Yung Chen, "*Self-tuning Gains of PI Controllers for Current Control in a PMSM*" 5th IEEE Conference on Industrial Electronics and Applications, 2010, PP 1282-1286

[13] R. Swaroop, Bency George and P. K. Sadhu, "*A Novel Design for Automatic Tuning of PID Controller Using Sugeno Based Fuzzy Logic*" INTERNATIONAL JOURNAL OF COMPUTATIONAL COGNITION, 2010, PP 99-103

[14] Oyas Wahyunggoro, Nordin B Saad, "*Development of Fuzzy-Logic-Based Self Tuning PI Controller for Servomotor*" 10th Intl. Conf. on Control, Automation, Robotics and Vision, December 2008, PP 1545-1550

[15] Minarech Peter, Makys Pavol and Vittek Ján, "*PI-Controllers Determination for Vector Control Motion***"** Department of Power Electrical Systems, Faculty of Electrical Engineering, University of Zilina

[16] Finn Haugen, "'*Ziegler-Nichols' Closed-Loop Method*" July 2010, PP 1-7

[17] Ludovic A. Chretien, "*Position Sensorless Control of Non-Salient Permanent Magnet Synchronous Machines*" The Graduate Faculty of the University of Akron, May 2006

[18] Texas Instruments Europe, "*Field Orientated Control of 3-Phase AC-Motors*" Literature Number: BPRA073, February 1998

[19] H.Soleimani Bidgoli, M.R.Ghazanchaei, **"**Analysis of Fuzzy Control for Permanent Magnet Synchronous Motor" 24th International Power System Conference, 2009, pp 1-3

[20] Joe Sung Yu, Sun Mo Hwang, Chung-Yuen Won, "*Performance of Fuzzy-Logic-Based Vector Control for Permanent Magnet Synchronous Motor Used in Elevator Drive System"* The 30th Annual conference of the IEEE Industrial Electronics Society, 2004, pp 2679-2683

[21] Chunhua Zang, "*Vector controlled PMSM Drive based on Fuzzy Speed Controller*" 2nd International Conference on Industrial Mechatronics and Automation, 2010, pp 199-202

[22] Y.S. Kung and P.G. Huang, "*High Performance Position Controller for PMSM Drives Based on TMS320F2812 DSP*" 2004 IEEE CCA/ISIC/CACSD Joint Conferences, CCA Proceedings, vol.I, pp. 290~295, September 2~4, 2004.

[23] Erwan Simon, "*Implementation of a Speed Field Oriented Control of 3-phase PMSM Motor using TMS320F240*" Texas Instruments Application Report SPRA588

[24] Shin-Hung Chang, Member IEEE, Pin-Yung Chen, "*Self-tuning Gains of PI Controllers for Current Control in a PMSM*" 2010 5th IEEE Conference on Industrial Electronics and Applicationsis, 2010, PP1282-1286

[25] National-Instruments, NI Developer zone, "*Optical Encoder Fundamentals*," www.opticalencoders.com

[26] *Dereje Shibeshi, "DSP Based Field Weakening Control of PMSM"* AAiT, School of Graduate studies, Department of Electrical and Computer Eng., 2007

[27] Alberto J. Pollmann, "*Software Pulsewidth Modulation for PM Control of AC Drives*", IEEE 1986 Transactions on industry applications, Vol. IA- 22, NO.4, July/August 1986

[28] P. Pillay and R. Krishnan, "*Modelling of Permanent Magnet Motor Drives*," *Industrial Electronics, IEEE Transactions on*, vol. 35, pp. 537-541, 1988

[29] Ying-Shieh Kung, Chung-Chun Huang, Kuan-Hsuan Tseng and Bill Su, "*Development of Sensorless PMSM Drive based on DSP Controller*", Digital Signal Processing Creative Design Contest, 2006

[30] Satoshi Ogasawara, Hirofumi Akagi, Akira Nabae, "*A novel PWM scheme of Voltage Source Inverters based on Space Vector Theory*", EPE Aachen 1989

[31] National-Instruments, NI Developer zone "*Quadrature Encoder Fundamentals*," http://zone.ni.com/devzone/cda/tut/p/id/4763

[32] Enrique L. Carrillo Arroyo, "*Modelling and simulation of Permanent Magnet Synchronous Motor System*" Universiy of Puerto Rico Mayaguez Campus, 2006

[33] www.opticalencoder.com

[34] Timthy J.Ross, "*Fuzzy Logic with Engineering Applications*" University of New Mexico, John Wiley & sons, Ltd, 2004

[35] Education for engineers, "fundamentals of PID control," PDHengineer.com, 2003

Appendix A

THE GENERATED C-CODE OF THE CONTROLLER ALGORITHM

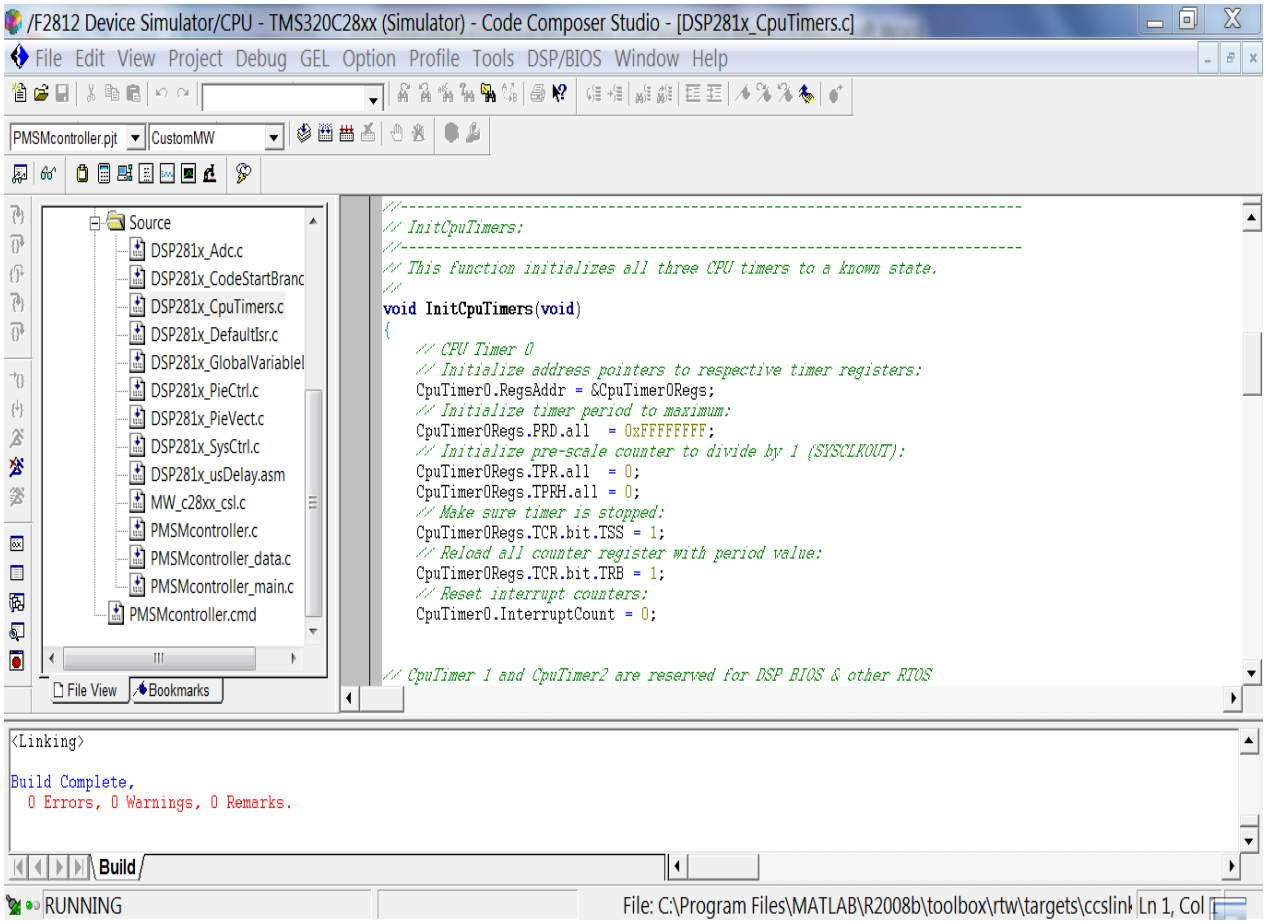

Appendix B

SPMSM PARAMETERS

Table B1: PMSM Motor Parameters.

Parameters	Values	Parameters	Values
Number of poles (p)	2x4	Friction (B)	0.00005396N.m/(rad/s)
Inductance (L_d=L_q)	$8.5\text{x}10^{-3}$H	PM magnetic flux (Ψ_m)	0.175ωb
Stator resistance	2.875Ω	Rotor Inertia (J)	0.0008Kg.m^2
Rated Power	0.7kw		